ORNL/TM-2016/291
CRADA/NFE-07-01054

High Efficiency Water Heating Technology Development—Final Report, Part II: CO_2 and Absorption-Based Residential Heat Pump Water Heater Development

Kyle R. Gluesenkamp
Viral Patel
Omar Abdelaziz
Bracha Mandel
Valmor deAlmeida

March 2017

OAK RIDGE NATIONAL LABORATORY
MANAGED BY UT-BATTELLE FOR THE US DEPARTMENT OF ENERGY

ORNL/TM-2016/291
CRADA/NFE-07-01054

Energy and Transportation Science Division

HIGH EFFICIENCY WATER HEATING TECHNOLOGY DEVELOPMENT – FINAL REPORT, PART II: CO_2 AND ABSORPTION-BASED RESIDENTIAL HEAT PUMP WATER HEATER DEVELOPMENT

Kyle Gluesenkamp
Viral Patel
Omar Abdelaziz
Bracha Mandel
Valmor deAlmeida

Date Published: March 2017

Prepared by
OAK RIDGE NATIONAL LABORATORY
Oak Ridge, Tennessee 37831-6283
managed by
UT-BATTELLE, LLC
for the
US DEPARTMENT OF ENERGY
under contract DE-AC05-00OR22725

CONTENTS

LIST OF FIGURES v
LIST OF TABLES vi
NOMENCLATURE vii
ABSTRACT AND STATEMENT OF OBJECTIVES 1
1. US RESIDENTIAL WATER HEATERS BACKGROUND 1
2. TECHNICAL DISCUSSION OF WORK PERFORMED BY ALL PARTIES 2
2.1 CARBON DIOXIDE HEAT PUMP WATER HEATER 2
2.1.1 Overview 3
2.1.2 Design Challenges for WAHX for Transcritical HPWH 6
2.1.3 CFD-Aided Design of Wrap-around Gas Cooler 10
2.1.4 Charge Management and Control Strategy Development 16
2.1.5 Experimental Evaluations of FHR, EF, UEF 16
2.2 ABSORPTION HPWH 26
2.2.1 Glycol-Based Anticrystallization Additive 34
2.2.2 Operational Strategies to Avoid Crystallization 34
2.2.3 HVAC Burden 36
2.2.4 Prototype Development 37
3. INVENTIONS AND COMMUNICATIONS 44
4. COMMERCIALIZATION POSSIBILITIES 46
5. References 46

LIST OF FIGURES

Figure 1. In the United States, most water heaters are installed in conditioned or semiconditioned spaces. 1
Figure 2. EcoCute configuration (*left*) and current project configuration (*right*). 4
Figure 3. Comparison of external and WAHX. 4
Figure 4. Timeline of CO_2 HPWH development. 5
Figure 5. Pressure-enthalpy cycle diagram for a CO_2 HPWH. 6
Figure 6. Refrigerant-side temperature profiles for stratified(*left*) and uniform (*right*) water tank temperature profiles and subcritical (*above*) versus supercritical (*below*) heat rejection. 7
Figure 7. Temperature-enthalpy cycle diagram for a CO_2 HPWH, with counterflow external HX process superimposed 8
Figure 8. Experimental data recorded over a 12 h period shows the minimal degradation in tank stratification during standby. 9
Figure 9. Temperature-enthalpy cycle diagram for a CO_2 HPWH with example tank water temperature profile. 10
Figure 10. Closeups of CFD mesh used in the analysis of WAGC. 11
Figure 11. Governing equations of fluid flow and heat transfer. 12
Figure 12. CFD validation methodology. 13
Figure 13. Design study using CFD. 14
Figure 14. Dramatic improvements in approach temperature were achieved by successive prototype WAHX designs. 15
Figure 15. Optimization of fixed charge of CO_2. 16
Figure 16. Water temperatures and compressor power for EF test on 01/28/2014 (EF=1.74), WAGC2. 18
Figure 17. WAGC CO_2 temperatures, water tank temperatures, COP, and compressor outlet/evaporator inlet pressures for EF test on 01/28/2014 (EF = 1.74), WAGC2. 19
Figure 18. Water temperatures and compressor power for EF test on 03/27/2014 (EF = 2.11), WAGC3. 19
Figure 19. WAGC CO_2 temperatures, water tank temperatures, COP, and compressor outlet/evaporator inlet pressures for EF test on 03/27/2014 (EF = 2.11), WAGC3. 20
Figure 20. WAGC CO_2 temperatures, water tank temperatures, COP and compressor outlet pressure versus gas cooler outlet temperature for heat-up test (1,100 g charge) on 05/21/2014. 21
Figure 21. WAGC CO_2 temperatures, water tank temperatures, COP and compressor outlet pressure versus gas cooler outlet temperature for heat-up test (1,050 g charge) on 06/03/2014. 22
Figure 22. WAGC CO_2 temperatures, water tank temperatures, COP and compressor outlet pressure versus gas cooler outlet temperature for heat-up test (1,205 g charge) on 12/17/2014. 23
Figure 23. Water temperatures and compressor power for EF test on 12/18/2014 (EF = 1.986). 23
Figure 24. WAGC CO_2 temperatures, water tank temperatures, COP and compressor outlet/evaporator inlet pressures for EF test on 12/18/2014 (EF = 1.986). 24
Figure 25. Water temperatures and compressor power for FHR test on 02/13/2015. 24
Figure 26. WAGC CO_2 temperatures and water tank temperatures for FHR test on 02/13/2015. 25
Figure 27.Water temperatures and compressor power for UEF test on 02/24/2015 (UEF = 2.11). 25
Figure 28. WAGC CO_2 temperatures, water tank temperatures, compressor outlet pressure versus gas cooler outlet temperature and compressor outlet/evaporator inlet pressures for UEF test on 02/24/2015 (UEF = 2.11). 26
Figure 29. Energy savings for gas heat pump water heaters. 27

Figure 30. Site and source EF for various water heating technologies. 27
Figure 31. Absorption HPWH technology has the potential to leapfrog the existing Pareto set of technologies by maximizing savings and minimizing installed retrofit cost. 28
Figure 32. The payback period for a $300 postincentive installed cost premium is favorable in many regions of the United States. 29
Figure 33. The conventional absorption process flow involves a solution HX transferring heat from the salty solution to the dilute, weak solution. 30
Figure 34. The ideal process flow for an absorption water heater typically involves cooling the absorber and condenser in series, with the condenser operating at the higher temperature..... 31
Figure 35. In a novel configuration, the process flow was modified so the hot solution heats the process water directly, which serves to lower the absorber temperature as much as possible. 32
Figure 36. In the novel semi-open architecture, the evaporator component is eliminated..... 33
Figure 37. The semi-open membrane-based ionic liquid absorption system addresses key challenges faced by absorption heat pump water heating technology. 33
Figure 38. Dühring solubility figure for the three mass ratios of 1,2-propanediol investigated. 34
Figure 39. The amount of heat drawn from the conditioned space, or HVAC burden, of electric (*left*) HPWHs is much greater than for gas (*right*) units. 37
Figure 40. HVAC burden of HPWHs as a function of EF. 37
Figure 41. Prototype based on water/LiBr in an ORNL lab. 38
Figure 42. Drawing of revised absorber used in 2nd generation water/LiBr prototype. 39
Figure 43. Investigation of stainless steel surface treatments to maximize wettability with salt solution..... 40
Figure 44. Last generation water/LiBr prototype..... 41
Figure 45. Tank temperatures during experimental heat up test with water/LiBr absorption prototype. 42
Figure 46. Membrane surface of condenser (*left*) and absorber (*right*). 42
Figure 47. Example pattern used to promote laminar mixing of the solution to enhance mass transfer. 43
Figure 48. Cross section of semi-open absorption architecture. 43
Table 5. Advantages of semi-open sorption systems 43

LIST OF TABLES

Table 1.Efficiencies and costs of existing water heating technologies 2
Table 2. Series of successive CO_2 HPWH prototypes 5
Table 3. Test result summary for generation 2, 3a, and 3b prototypes 18
Table 4. Operational crystallization challenges 36

NOMENCLATURE

CFD	computational fluid dynamics
COP	coefficient of performance
DHW	domestic hot water
DOE	Department of Energy
EF	energy factor
FHR	first hour rating
GWP	global warming potential
HFC	hydrofluorocarbon
HPWH	heat pump water heater
HVAC	heating, ventilation, and air conditioning
HX	heat exchanger
IHX	internal heat exchanger
K	Kelvin
RH	relative humidity
UDF	user-defined function
UEF	uniform energy factor
WAGC	wrap-around gas cooler
WAHX	wrap-around heat exchanger

ABSTRACT AND STATEMENT OF OBJECTIVES

The two objectives of this project were to

1. demonstrate an affordable path to an ENERGY STAR®–qualified electric heat pump water heater (HPWH) based on low-global warming potential (GWP) CO_2 refrigerant, and

2. demonstrate an affordable path to a gas-fired absorption-based heat pump water heater with a gas energy factor (EF) greater than 1.0.

The first objective has been met, and the project has identified a promising low-cost option capable of meeting the second objective. This report documents the process followed and results obtained in addressing these objectives.

1. US RESIDENTIAL WATER HEATERS BACKGROUND

In the United States, roughly half of residential water heating is powered by natural gas and the other half by electricity. Most units are based around a water storage tank, and the remainder are tankless, which are also known as instantaneous. The gas units available today combust natural gas and directly transfer the combustion heat to water, and most of the electric units use electric resistance elements to convert electricity directly into heat. There is an emerging category of electric HPWHs, which represent about 46,000 unit shipments in calendar year 2014. Gas HPWH are not yet available on the market.

Most of the market is for retrofits, and retrofits typically require a replacement unit to be installed in the same location as the old unit. Heat pump water heaters, whether gas- or electric-driven, benefit from warmer surrounding air temperature, so the installation location is important. Figure 1 shows the majority of water heaters in the United States are installed in conditioned or semiconditioned spaces; although, a significant fraction (43%) are in garages, crawlspaces, or outdoor closets. Some garage locations may be considered semiconditioned and may be at risk of occasional subfreezing temperatures in some climates.

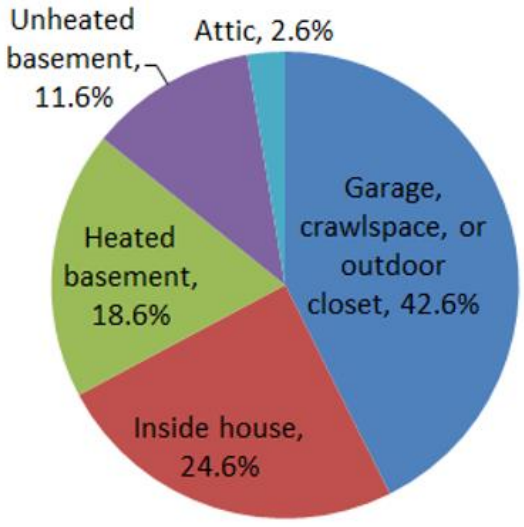

Figure 1. In the United States, most water heaters are installed in conditioned or semiconditioned spaces.

The main currently available storage water heating technologies are shown in Table 1 from the 2010 DOE technical support document for water heater minimum efficiency rulemaking (DOE 2010). It is important to note that the electric HPWH can demonstrate a reasonable 3.8 y payback compared with the baseline electric resistance unit. This is enabled by the relatively high monthly energy cost of operating an electric water heater (typically $20–$40/mo), and the very large jump in efficiency between resistance and heat pump models (0.90–2.35 EF). In contrast, a gas water heater has a comparatively lower annual energy cost (typically $10–$15/mo), and a slight improvement in efficiency between condensing and noncondensing technology (0.65–0.77 EF). There is less opportunity for cost savings, and the payback period for gas condensing storage water heating is relatively unfavorable at about 12 y. This poor payback for gas condensing technology represents an opportunity for gas HPWHs, which may be able to leapfrog gas condensing technology if they are able to provide a more dramatic improvement in EF (e.g., 0.65–1.0) and keep the installed cost relatively low.

Table 1.Efficiencies and costs of existing water heating technologies

Type	EF	Retail [$US]	Installation [$US]	Payback period
Electric resistance	0.90	$300	$280	—
Electric HPWH	2.35	$1,050	$530	**3.8 y**
Gas, noncondensing	0.65	$410	$625	—
Gas, condensing	0.77	$960	$900	**12.1 y**

Data source: DOE, Final Rule Analytical Tools (2011).

Improving energy efficiency in water heating equipment is important to the nation's energy strategies. According to the Department of Energy's (DOE) 2011 Buildings Energy Data Book (DOE 2012), water heating in residential and commercial buildings accounted for about 9% of US buildings primary energy consumption in 2010: 4.1% from electricity, 4.3% from natural gas, and the rest from oil, liquefied petroleum gas, and solar (DOE 2012). HPWH technology is a significant breakthrough in energy efficiency. Electric HPWH technology has shown acceptable payback period with proper incentives, and successful market penetration is emerging. However, current electric HPWHs use refrigerants with relatively high GWP. Furthermore, current system designs depend greatly on the backup resistance heaters when the ambient temperature is below freezing or when hot water demand increases. Finally, the performance greatly degrades as the hot water set point temperature exceeds 60°C. Such temperatures are desirable for facilitating residential and commercial demand response strategies, as well as many commercial sanitary applications.

2. TECHNICAL DISCUSSION OF WORK PERFORMED BY ALL PARTIES

2.1 CARBON DIOXIDE HEAT PUMP WATER HEATER

Carbon dioxide heat pump water heating uses a refrigerant with a GWP of 1.0 and zero ozone depletion potential coupled with a potential for higher efficiency under certain conditions (e.g., hot water set points above 60°C or very low ambient temperatures). The CO_2 HPWH cycle is transcritical, operating at much higher temperatures and pressures than conventional subcritical cycles. The transcritical cycle operation provides a large continuous temperature glide and can offer a higher service temperature with limited capacity loss. Carbon dioxide HPWH systems are currently used in Asia and Europe for water heating. Development is needed to configure the technology for replacement and integration in the US water heating market.

Thermodynamically, transcritical CO_2 cycles hve inherent advantages, where very large temperature lifts are required with a large temperature glide for the fluid being heated. However, under the most common residential water heating conditions, the transcritical CO_2 cycle is inherently less efficient than conventional subcritical vapor compression cycles. Much research has focused on improving the performance of CO_2 systems using system enhancements such as work-recovery components. Increasing the performance of compressors and heat exchangers (HXs) is also vital to making CO_2 a viable heat pump technology. With the pending US plan to phase down HFC refrigerants and the benefits of using a commonly available, nontoxic, nonflammable refrigerant, CO_2 systems are compelling for future applications.

EcoCute carbon dioxide-based HPWHs, developed and widely used in Japan, are highly efficient, but not suitable for the US market because of their high cost. A key enabler of low-cost systems for the US market would be a wrap-around gas cooler (WAGC). A WAGC eliminates the need for a water pump and uses an inexpensive tube wrapped around the tank instead of an expensive, water fouling–prone plate HX. The wrap-around heat exchanger (WAHX) is already implemented in one of the most successful HFC-based residential HPWH products available in the United States. As discussed in the next section, the design of a WAGC in a transcritical HPWH has unique challenges compared with a subcritical HPWH. The primary focus of this report is the description of a methodology to develop an optimal WAGC design for transcritical CO_2 HPWHs.

2.1.1 Overview

Carbon dioxide systems are on the market today in large numbers in Japan under the EcoCute name. These systems have very high efficiency, but also high cost. This is partly because of the split nature of the design (separate indoor and outdoor units), as well as the use of high efficiency variable speed scroll compressor, electronic expansion valve, external brazed plate HX, variable speed water pump, a large water storage volume, and sophisticated controls. To configure a CO_2 system for the highly cost-sensitive US market, a lower cost system design is required. Figure 2 contrasts the EcoCute configuration with a schematic of the configuration developed in this project. The low-cost configuration envisioned would be a one-piece unit with the CO_2 heat pump section mounted on top of the water tank as is done for the top selling electric HPWHs now on the market.

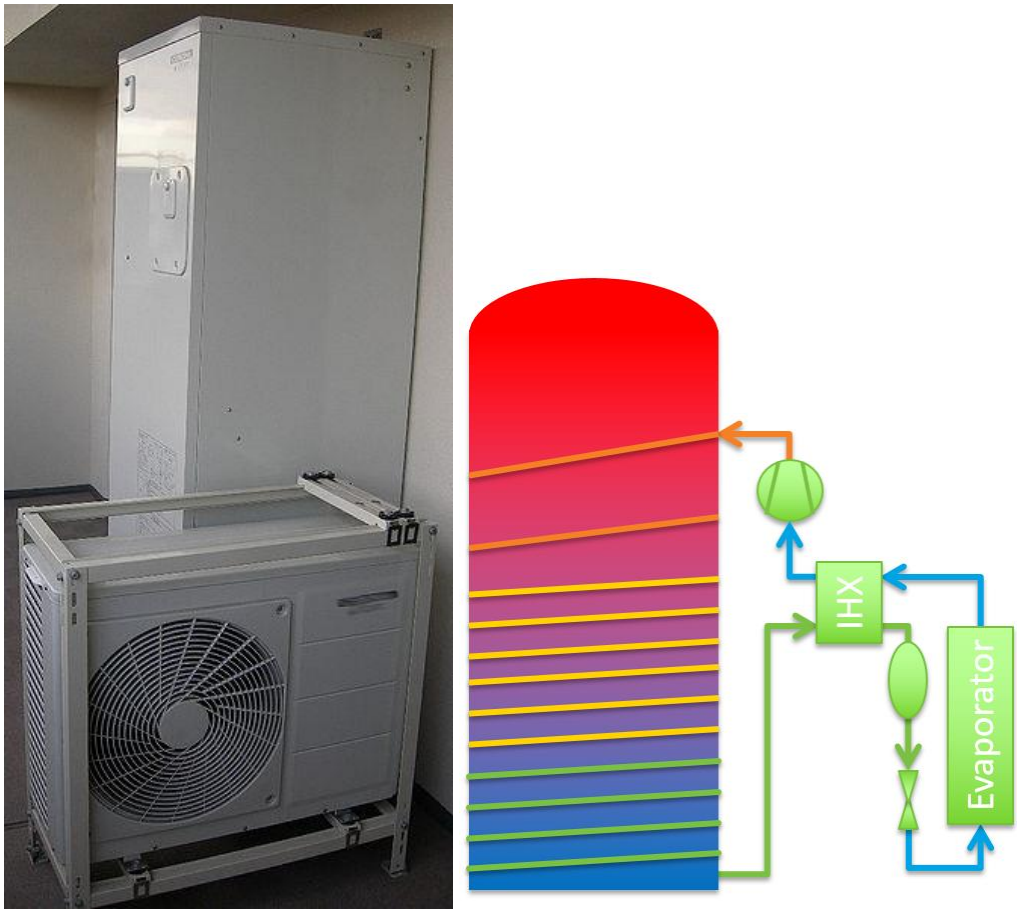

Figure 2. EcoCute configuration (*left*) and current project configuration (*right*).

Key to enabling the lower cost design is the WAHX. Characteristics of the external (brazed plate) and WAHX are compared in Figure 3.

Characteristic	External heat exchanger	Wrap-around heat exchanger
Cost	✗ High	✓ Low
Water fouling	✗ Significant challenge	✓ None
Water pump	✗ Required	✓ Not required
Additional tank water inlet/outlet ports	✗ Required	✓ Not required
Performance	✓ Good	? Needs research

Figure 3. Comparison of external and WAHX.

To understand and design the best coil wrapping pattern, computational fluid dynamics (CFD) modeling and a series of successive prototypes were developed for CO_2. The CO_2 prototypes are detailed in Table 2 and placed on a timeline in Figure 4.

Table 2. Series of successive CO_2 HPWH prototypes

Prototype generation	WAGC	Tank	Compressor	Other notes	WAGC $T_{approach}$	FHR/EF/UEF
Gen. 1a FY 2012	1st (wrapped by hand)	A* (50 gal)	A†		>10 K	Not evaluated
Gen. 1b FY 2012	1st (extended length)				10 K	Not evaluated
Gen. 2 FY 2014 Q1	2nd (wrapped by mechanical winder)	B* (50 gal)	B†	Improved WAHX	5 K	EF = 1.74
Gen. 3a FY 2014 Q2	3rd (wrapped by mechanical winder)				2.5 K	FHR = 73 EF = 2.11
Gen.3b FY 2015 Q1				Redesigned evaporator, IHX	2.5 K	FHR = 73 EF = 1.99 UEF‡ = 2.11

*Tanks A and B were both of the same nominal volume, but had slightly different internal shapes
†Compressors A and B were both prototypes provided under material transfer agreements
‡5 of 12 draws had volume discrepancies, each of less than 3.2%
Note: EF = energy factor, FHR= first hour rating; IHX = internal heat exchanger; UEF = uniform energy factor

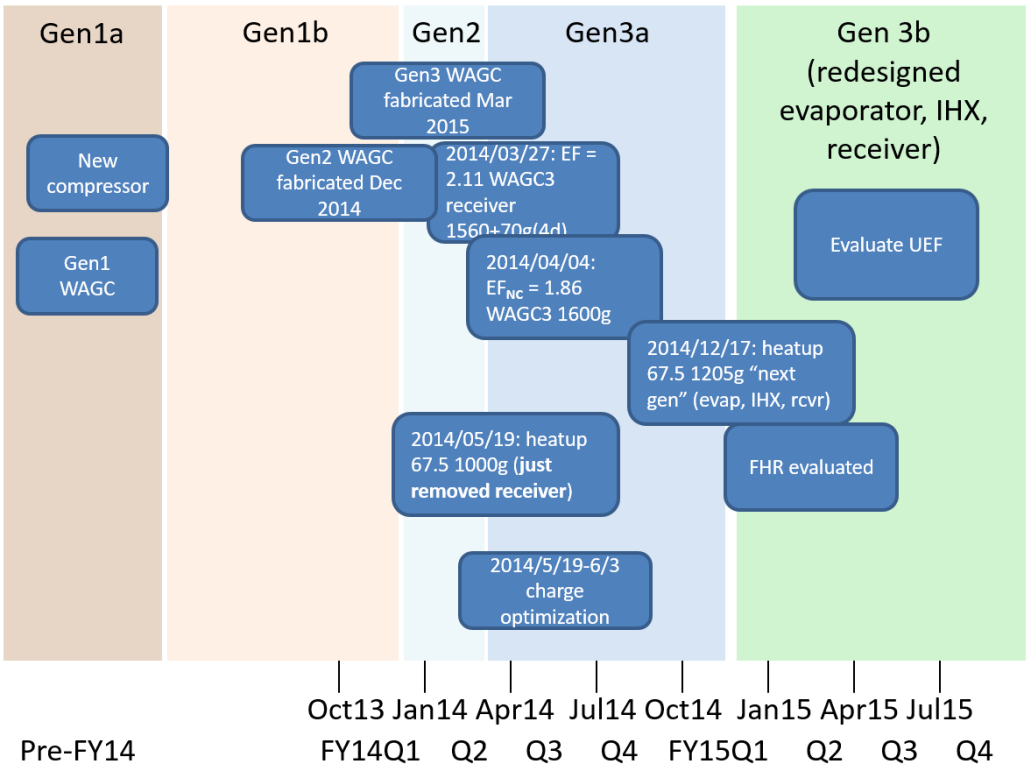

Figure 4. Timeline of CO_2 HPWH development.

2.1.2 Design Challenges for WAHX for Transcritical HPWH

The difference in performance between the external and WAHX is illustrated in a series of figures. Figure 5 shows a vapor compression cycle in a pressure enthalpy diagram. Since the critical temperature of CO_2 is 31.1°C (88°F), some of the cycle is subcritical and some is supercritical. Consequently, the cycle is called "transcritical."

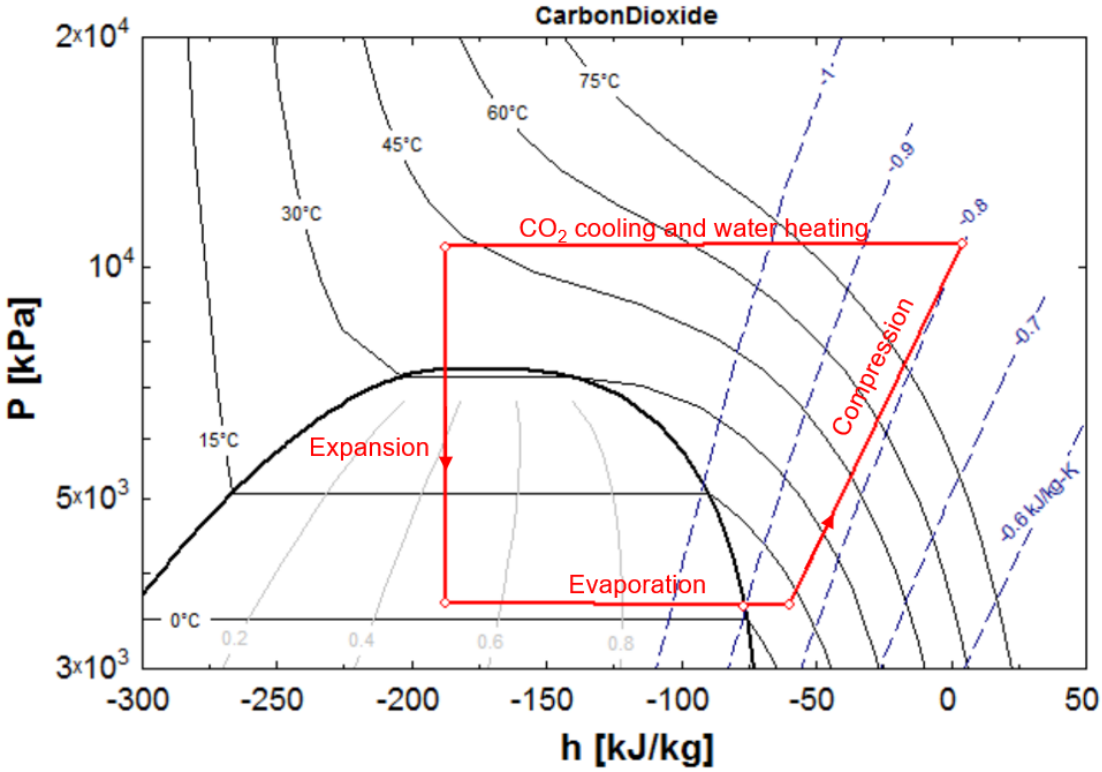

Figure 5. Pressure-enthalpy cycle diagram for a CO_2 HPWH.

The significance of the CO_2 cooling while supercritical is that it does not condense at a constant temperature like the traditional reverse Rankine cycle. The large change in temperature it undergoes as it cools is called the "glide." Reading the isotherms in Figure 5, the CO_2 undergoes a glide from well in excess of 75°C down to about 43°C as it transfers heat to water.

Figure 6 qualitatively demonstrates a fundamental difference between the subcritical and transcritical cycles. The figure compares refrigerant-side temperature profiles for two tank temperature profiles with the same average tank temperature. The refrigerant temperature leaving the condenser or gas cooler is closely related to cycle performance, with lower refrigerant outlet temperatures yielding a higher coefficient of performance (COP) and higher capacity.

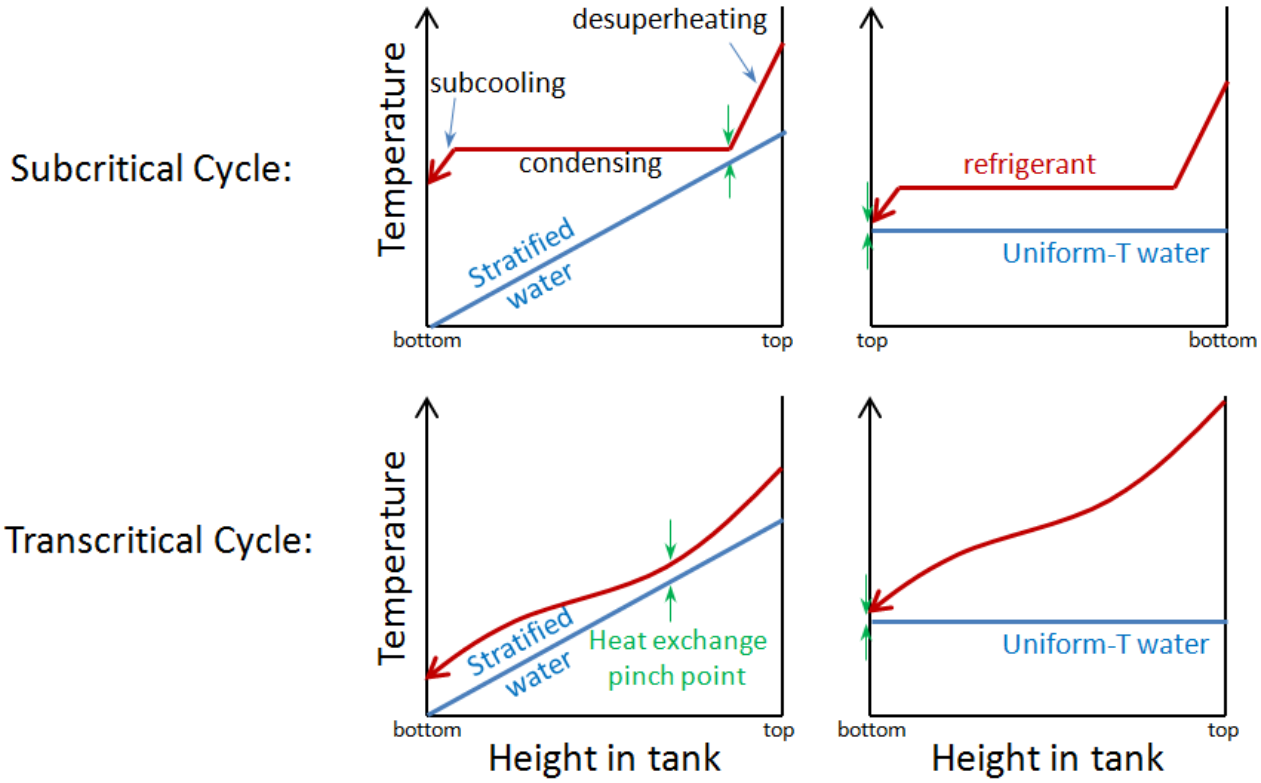

Figure 6. Refrigerant-side temperature profiles for stratified(*left*) and uniform (*right*) water tank temperature profiles and subcritical (*above*) versus supercritical (*below*) heat rejection.

For the same average tank water temperature, a subcritical cycle can benefit from a uniform water temperature profile. Since the refrigerant temperature must be above the water temperature at all times, the refrigerant temperature is constant through the majority of the HX coil length. Roughly speaking, the refrigerant outlet temperature will be close to the hottest water temperature in a subcritical cycle.

In contrast, transcritical cycles depend on stratification for efficient performance. With a stratified tank, the refrigerant outlet temperature can approach the coldest water temperature; with a mixed tank, the refrigerant outlet temperature must remain above the water temperature. The transcritical cycle is able to capitalize on the stratification; however, it is also critically dependent on stratification for acceptable performance.

The principles illustrated in Figure 6 are reflected in the design of commercially available products. Most of the HFC-based HPWHs in the United States use wrap-around condensers (WAHX), with the refrigerant entering the coil from the bottom of the tank and traveling up. This arrangement promotes large-scale natural convection of the water in the tank and leads to a uniform water temperature profile. In contrast, the transcritical EcoCute appliances pump water through an external gas cooler, and the hot water is charged to the top of the storage tank. Buoyancy forces maintain stratification in the tank, so cold water is always available to be drawn from the tank bottom into the gas cooler.

Designing a WAGC for a transcritical system means doing everything possible to promote stratification.Clearly the hottest tubes should start at the tank top and work their way down. However, many questions without intuitive answers remain:

- How high should the first tube be placed?

- How closely should the tubes be spaced?
- Should the spacing be even, or get closer or farther away toward the tank bottom?
- How many tubes should be used, and what diameter should they have?

These questions cannot be addressed in a cost effective way experimentally. Consequently, we devised a comprehensive modeling framework to optimize the WAGC design to achieve the best tank stratification and the highest possible EF.

As illustrated in Figure 7, this temperature glide can be effectively used in a counterflow external HX to heat water in a single pass from low to very high temperatures, in this case from about 27°C–84°C. With a conventional subcritical reverse Rankine cycle, this would require refrigerant condensing temperatures above 84°C. The CO_2 cycle will perform very poorly when the incoming cold water temperature rises too high, so it is important to maintain cold water in the water storage tank by maintaining temperature stratification.

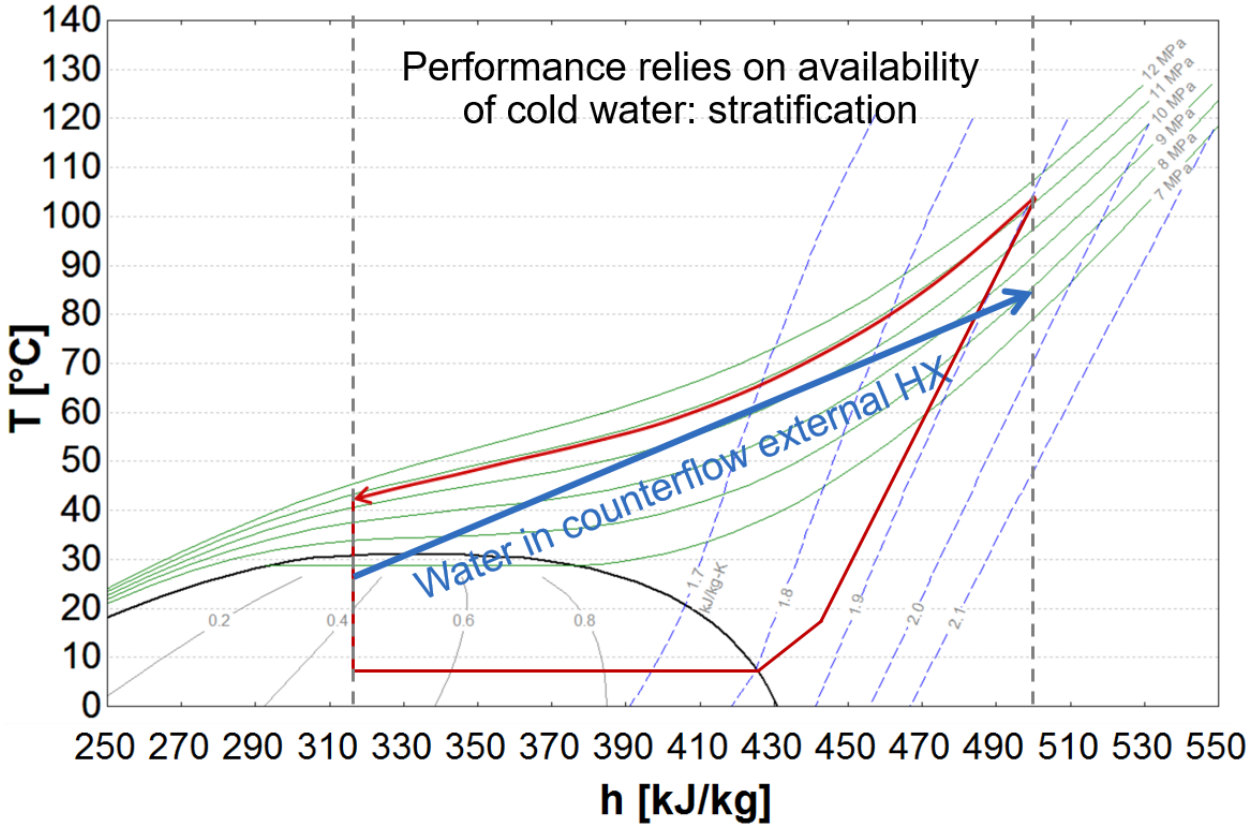

Figure 7. Temperature-enthalpy cycle diagram for a CO_2 HPWH, with counterflow external HX process superimposed

Fortunately, a natural property of insulated water tanks commonly used in water heaters is good passive maintenance of temperature stratification. Figure 8 shows experimentally measured temperature in an initially stratified residential water heater tank. Over a 12 h period, the tank loses heat through its insulation to the surroundings, but the hottest temperature in the tank stays well above the coldest.

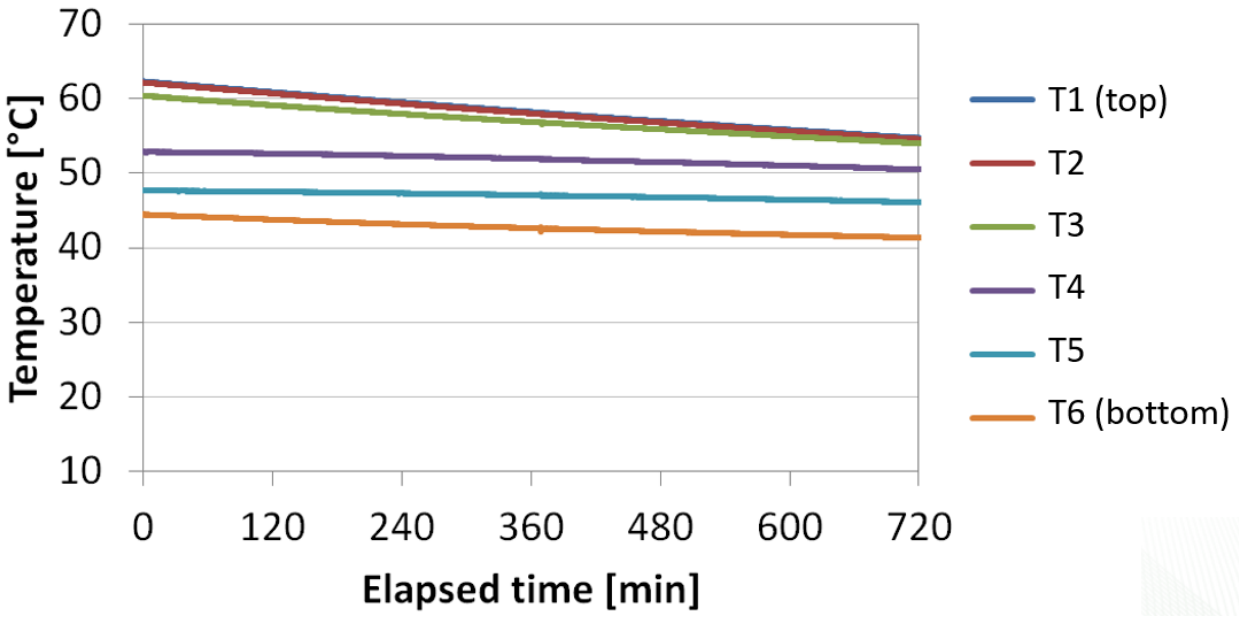

Figure 8. Experimental data recorded over a 12 h period shows the minimal degradation in tank stratification during standby.

It is straightforward to plot the temperature-enthalpy diagram a pure counterflow external HX (Figure 7): the water being heated follows a nearly straight line because it has a nearly constant specific heat capacity.

However, analyzing the lower-cost WAHX is less straightforward. Determining the water temperature in contact with each point in the CO_2 coil depends on the interaction of the vertical wrapping pattern of the coil, and the vertical water profile in tank (Figure 9). Furthermore, the vertical water profile in the tank is a function of the draw history, the heat pump run time history, and the coil wrapping pattern.

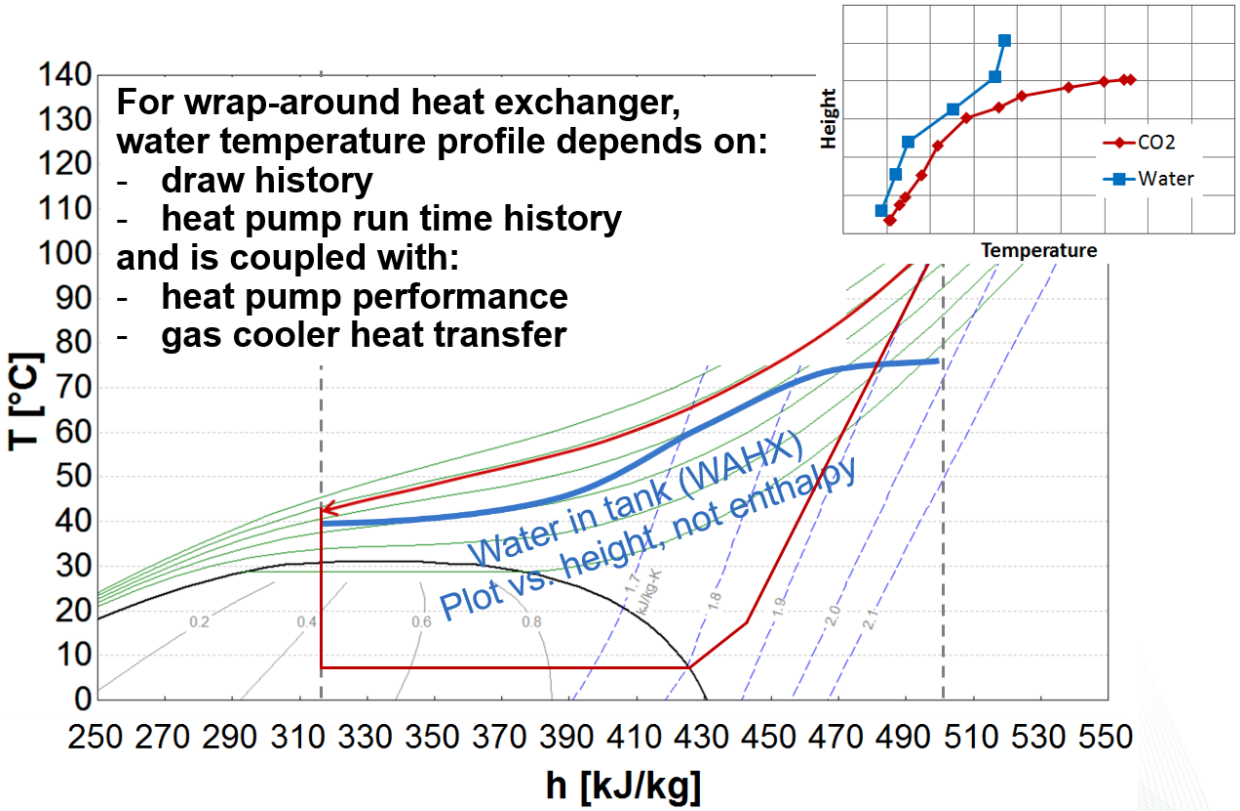

Figure 9. Temperature-enthalpy cycle diagram for a CO_2 HPWH with example tank water temperature profile. The inset shows experimentally measured data for height versus temperature.

2.1.3 CFD-Aided Design of Wrap-around Gas Cooler

A CFD-based investigation was conducted to aid in design of the WAGC wrapping pattern. A continuum mechanics modeling approach was pursued in this work to support experimental data acquisition on water heating and extend the validity of the design approach to optimize the coupled gas cooling and water heating process. In particular, the governing equations of laminar, buoyant, Newtonian, and incompressible fluids are stated and solved using the finite volume method as implemented by ANSYS Fluent. The nonisothermal equations of heat transport are solved for the fluid and solid materials in the model in a coupled fashion as described in the following subsections.

The water tank is assumed to be a cylindrical-like vessel wherein axisymmetry is enforced in the geometrical and mathematical model. Figure 10 shows closeups of the axisymmetric mesh used in ANSYS Fluent to model the geometry. A refined mesh was built using ANSYS meshing to resolve submillimeter flow and heat transport. The mesh is specially refined in the regions near the CO_2 coils, thermal paste, and vessel steel wall (brown region). The circles along the outside of the tank wall represent the CO_2 tubes. Not all tubes were active at once—a user-defined function in ANSYS allowed the team to assess different coil wrapping designs by selectively activating tubes in the mesh without having to modify the mesh between cases. This allowed evaluation of a larger number of cases.

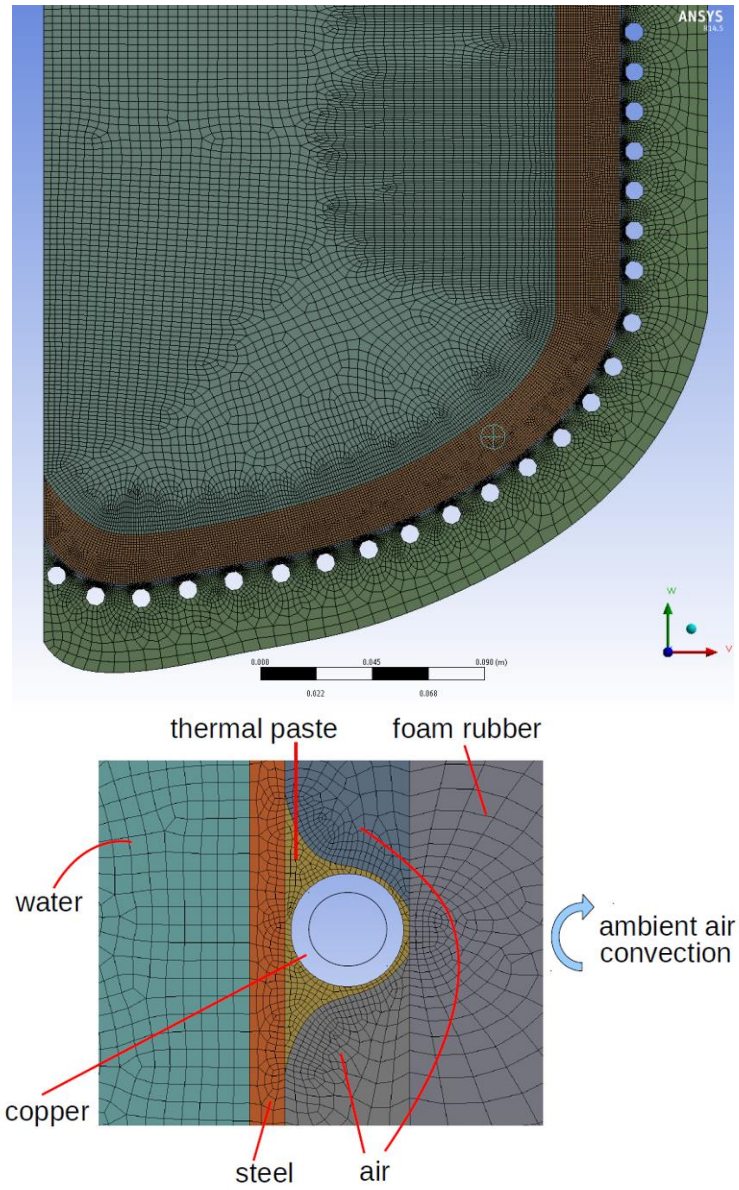

Figure 10. Closeups of CFD mesh used in the analysis of WAGC.

As previously mentioned, the equations of fluid flow and heat transfer adopted here employ buoyancy by means of a Boussinesq approximation (Figure 11).

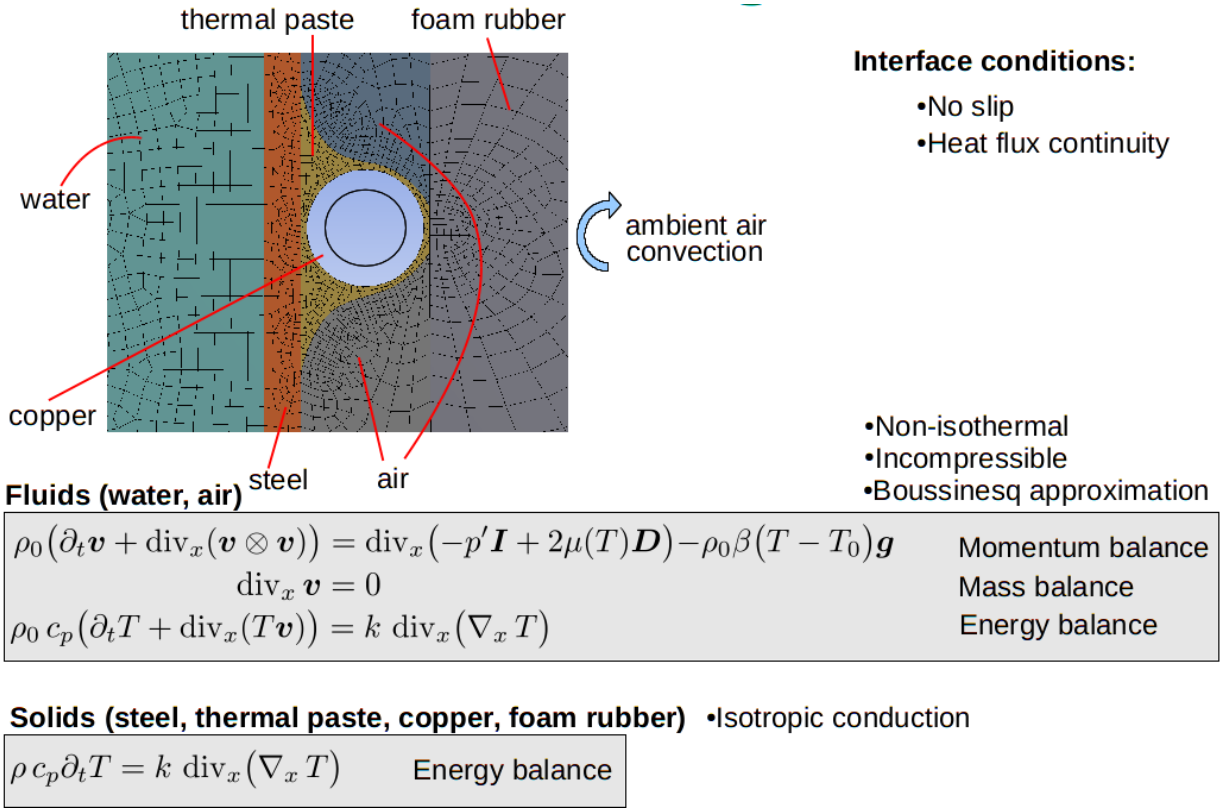

Figure 11. Governing equations of fluid flow and heat transfer.

To be useful, the model needed to be validated against experimental data. Standard thermophysical properties were used in the model for all solid materials and fluids. As illustrated in Figure 12, the notable exception is the thermal paste material used to mimic the contact resistance between the copper wrap around the coil and the steel tank. Here the thermal properties are adjusted to calibrate the simulation results with the experimental measurement previously obtained. This gives the model a tunable contact resistance between the tube and tank walls, since this interface cannot be reliably characterized from geometric measurements alone. Only one parameter was used as a "calibration parameter."

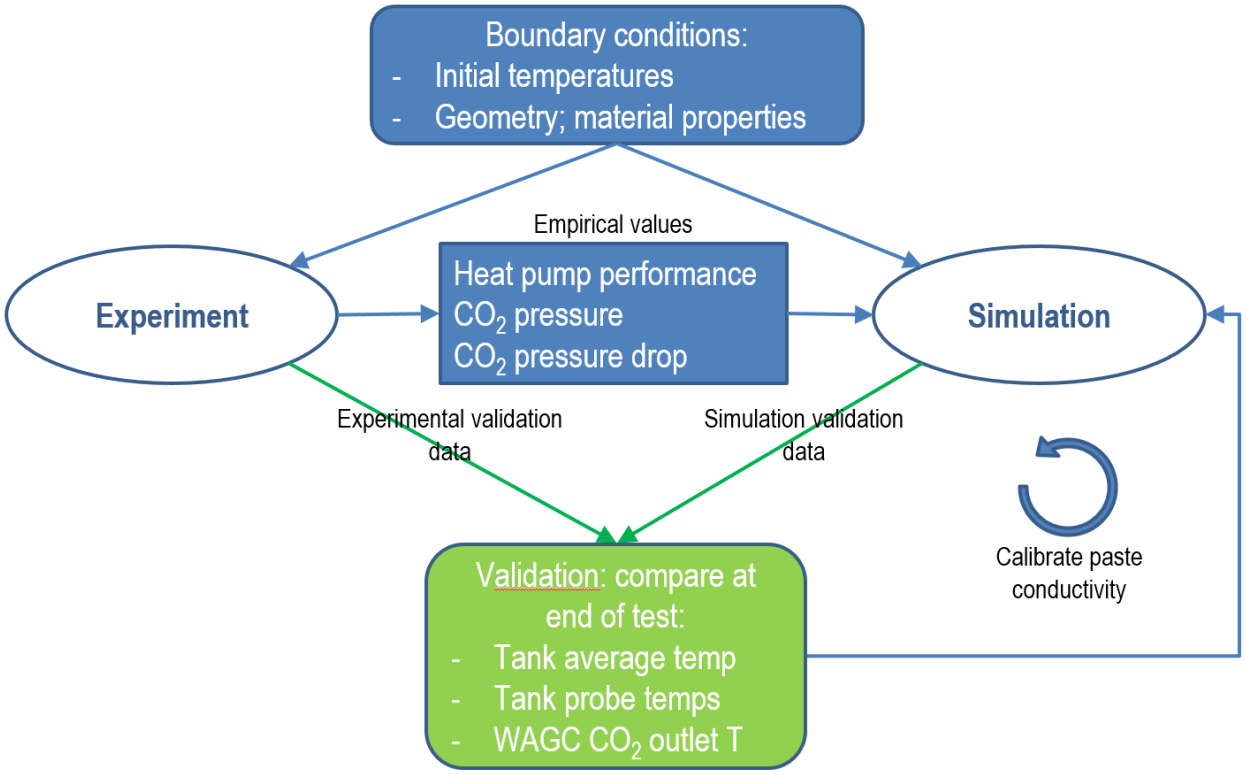

Figure 12. CFD validation methodology.

Once validated by experimental data measured in the lab, CFD was used as a design tool to evaluate different wrap designs. Figure 13 shows a subset of the cases evaluated, and each star is plotted at the height of an active coil. Holding the number of wraps (i.e., tubing length) constant and varying the vertical placements of those tubes allowed simulated evaluation of different coil wrapping designs. The best design is the one that maximizes heat pump cycle efficiency. This is achieved when a given average tank water temperature was reached with the lowest amount of CO_2 temperature exiting the coil.

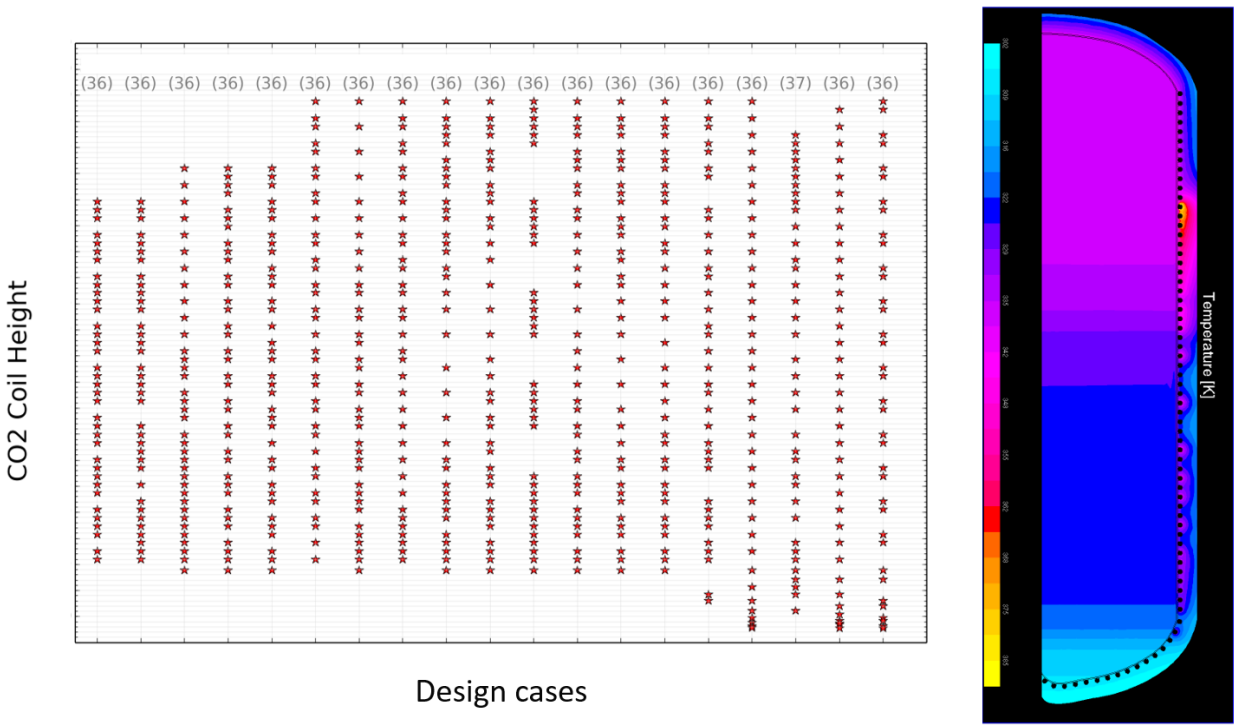

Figure 13. Design study using CFD.

This design approach proved successful. As detailed further below, Figure 14 summarizes the results achieved. The experimentally measured temperature approach over three prototype iterations was reduced from 10 K, to 5 K, to 2.5 K. This resulted in dramatic increases in the EF. Although it was not measured for the first prototype, it increased from 1.74 to 2.11 from the second to third generation.

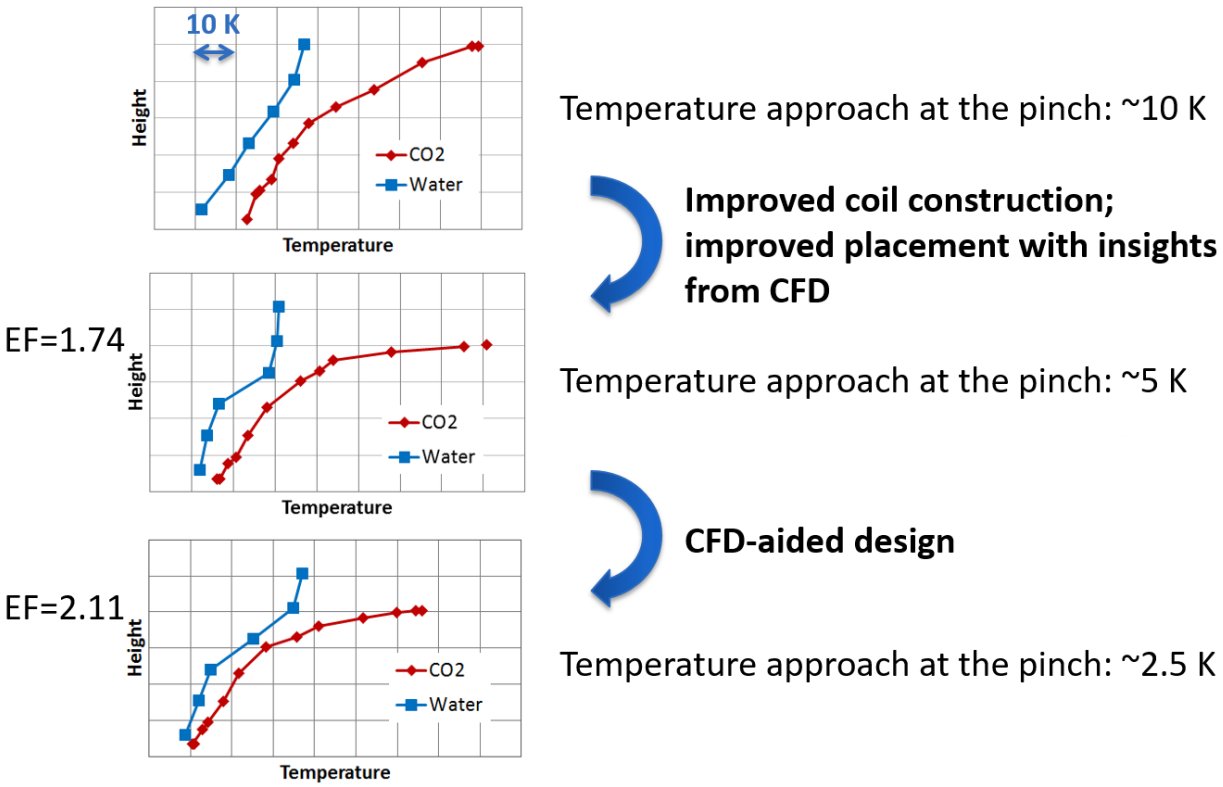

Figure 14. Dramatic improvements in approach temperature were achieved by successive prototype WAHX designs.

2.1.4 Charge Management and Control Strategy Development

The refrigerant charge was optimized through a series of experimental heat up tests, as shown in Figure 15. The optimum high side pressure, and the deviations from it that would result in a 10% penalty to COP, were determined by a modeling study. Then heat up tests were run experimentally at various charge levels to determine which charge would keep the system closest to the optimal high side pressure at a wide range of temperature conditions.

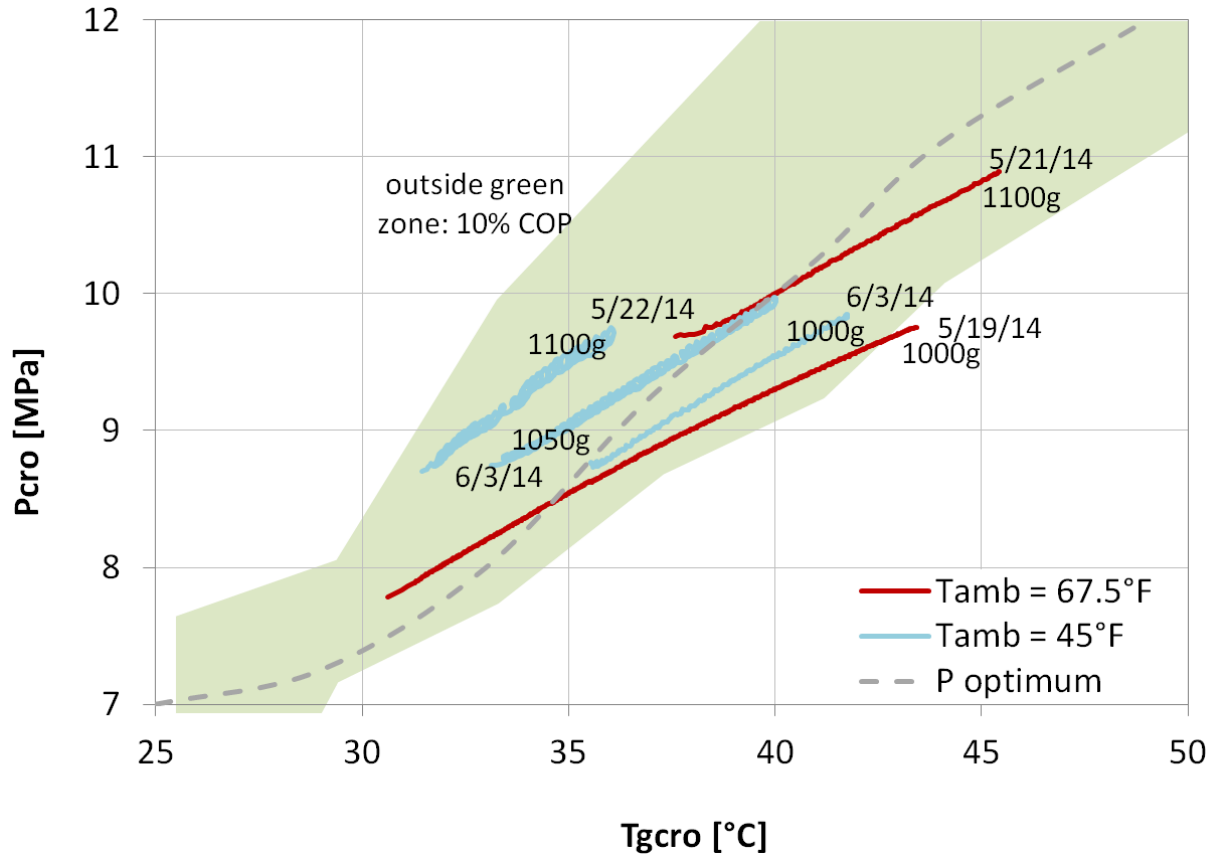

Figure 15. Optimization of fixed charge of CO_2.

2.1.5 Experimental Evaluations of FHR, EF, UEF

The second generation of the prototype includes the improved coil construction derived from CFD modeling. The receiver is removed in generation 3a. In the final prototype generation (3b), the IHX and evaporator were replaced, and a new auxiliary heater and mixing valve were added. A summary of the experimental first hour rating (FHR), EF, and UEF test results for the generation 2, 3a and 3b prototypes is given in

Table 3.

Table 3. Test result summary for generation 2, 3a, and 3b prototypes

Date	Test type	Generation	EF/UEF	CO_2 charge	Remarks
Generation 2 (improved coil)					
01/28/2014	EF	2	1.74	—	WAGC2—further design optimization with CFD after this test
03/27/2014	EF	2	2.11	1,560 g + 70 g	WAGC3 with different wrapping pattern
4/4/2014	EF_{NC}	2	1.86	1600 g	50.0°F, 60% RH (based on NEEA northern climate specification version 5.0)
Generation 3a (receiver removed)					
05/21/2014	Heat up	3a	—	1,100 g	67.5°F, 50% RH
06/03/2014	Heat up	3a	—	1,050 g	44.6°F, 40%–50% RH
Generation 3b (new IHX, evaporator, aux. heater, mixing valve)					
12/17/2014	Heat up	3b	—	1,205 g	67.7°F, 50% RH
12/18/2014	EF	3b	1.99	1,205 g	67.5°F, 50% RH
1/9/2015	EF_{NC}	3b	1.64	1,205 g	50.0°F, 60% RH (based on NEEA northern climate specification version 5.0)
02/13/2015	FHR	3b	—	—	FHR = 73.52, medium usage draw profile
02/24/2015	UEF	3b	2.11	—	5 of 12 draws slightly out of spec (all by less than 3.2%)
07/27/2016	UEF	3b	2.02	1,205 g	Mixing valve deactivated

Note: EF = energy factor, FHR= first hour rating; IHX = internal heat exchanger; RH = relative humidity; UEF = uniform energy factor

2.1.5.1 Generation 2 EF tests

Figure 16 through Figure 19 show the temperatures in the water tank (i.e., individual measurements from the thermocouple tree and average tank temperature), water supply and delivery temperatures (during draws), compressor power, WAGC CO_2 temperatures and compressor outlet pressure and temperature for the duration of two EF tests on the generation 2 prototype:

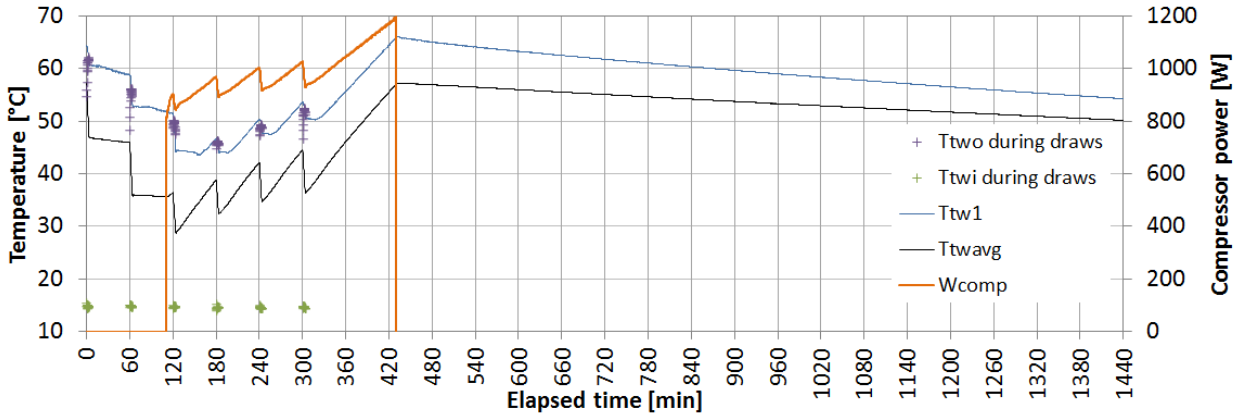

Figure 16. Water temperatures and compressor power for EF test on 01/28/2014 (EF=1.74), WAGC2.

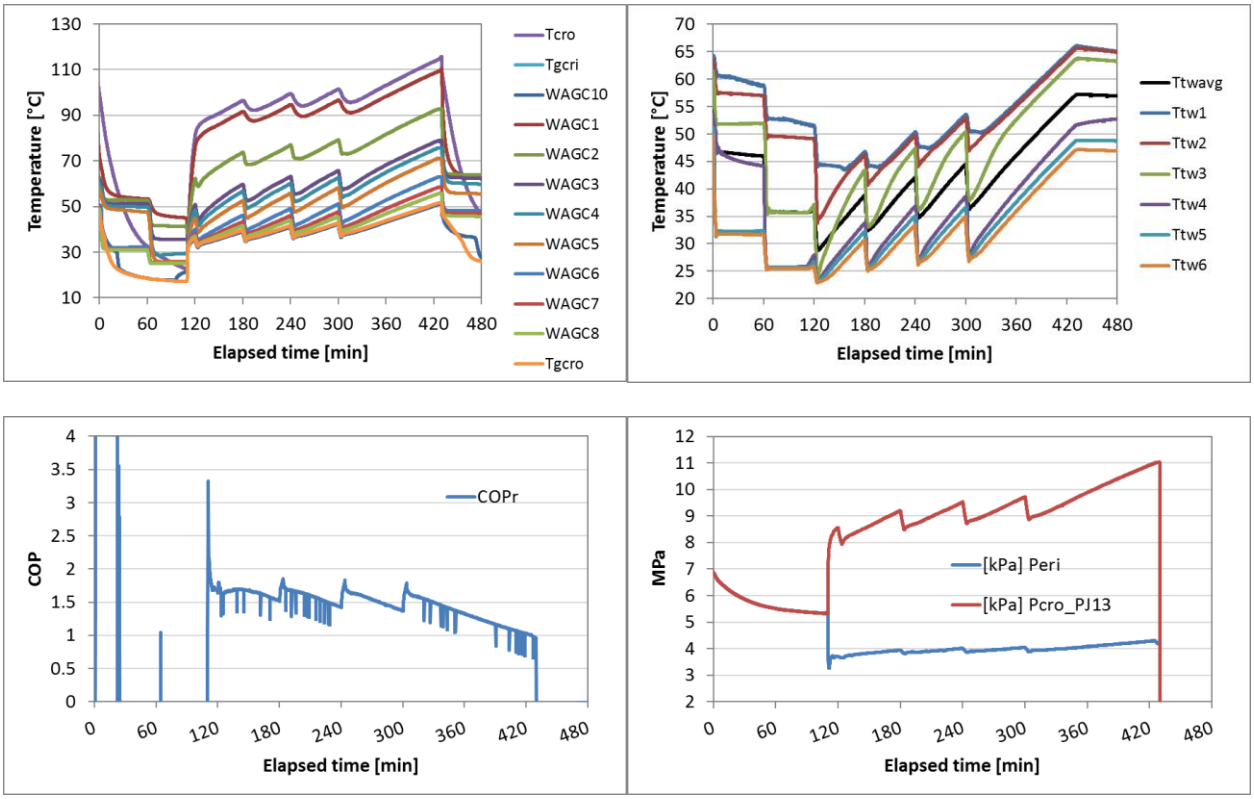

Figure 17. WAGC CO_2 temperatures, water tank temperatures, COP, and compressor outlet/evaporator inlet pressures for EF test on 01/28/2014 (EF = 1.74), WAGC2.

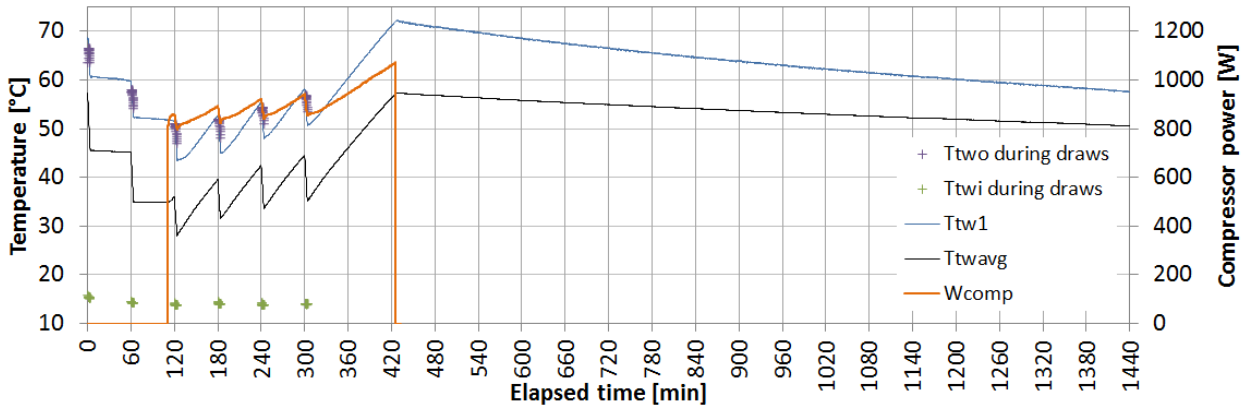

Figure 18. Water temperatures and compressor power for EF test on 03/27/2014 (EF = 2.11), WAGC3.

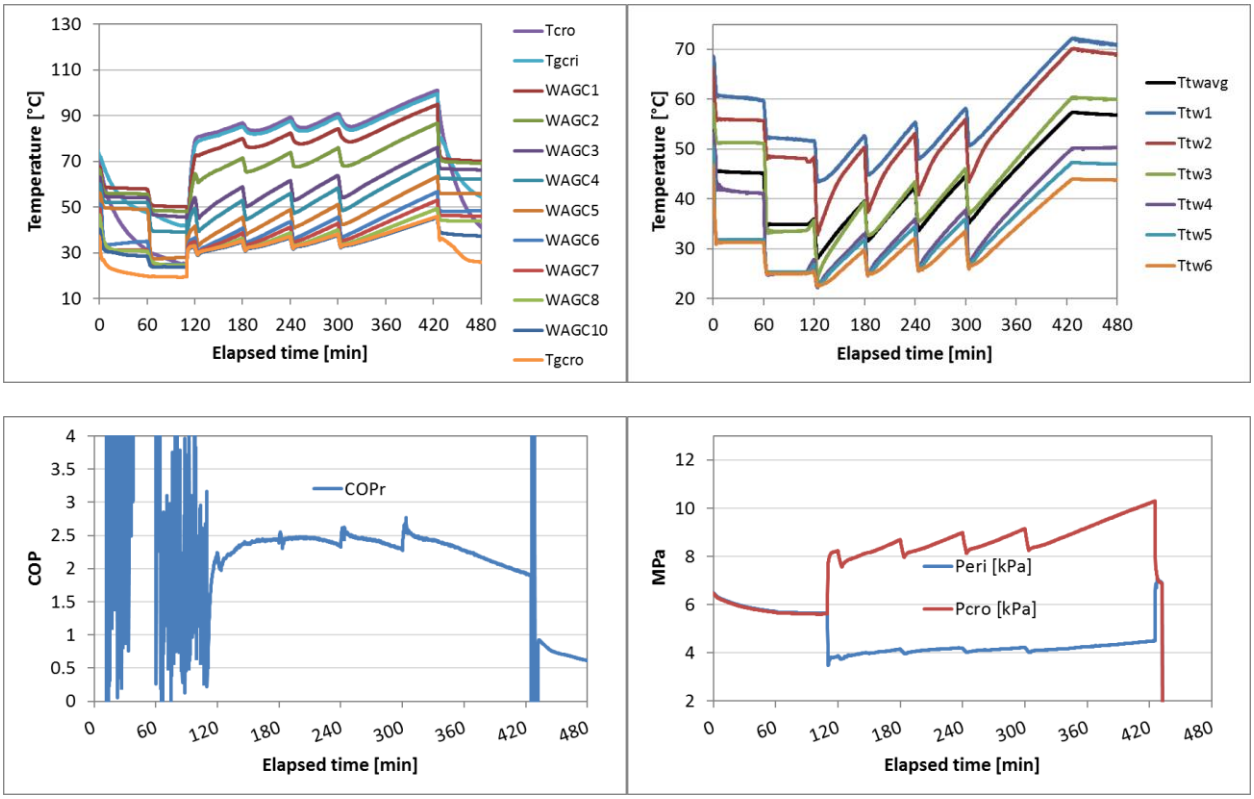

Figure 19. WAGC CO_2 temperatures, water tank temperatures, COP, and compressor outlet/evaporator inlet pressures for EF test on 03/27/2014 (EF = 2.11), WAGC3.

From the above graphs, we can see the reasons for the increase in the EF between the two tests resulting from the improved WAGC design: the approach between water tank temperature and WAGC temperature was minimized (Figure 14), the tank average and WAGC temperatures were increased, and the COP was increased. Additionally, insulation was added to the water tank before the 03/27/2014 test to reduce standby losses.

2.1.5.2 Gen. 3a heat-up tests

With the receiver removed from the experimental setup, heat-up tests were conducted from 05/19/2014 to 06/03/2014. The purpose of these was to determine the appropriate charge for the new system after the receiver had been removed. The results of two heat-up tests from 05/21/2014 and 06/03/2014 are shown in Figure 20 and Figure 21, respectively. The primary differences are the charge amount, ambient temperature, and relative humidity (RH) (67.5°F, 50% RH versus 44.6°F, 40%–50% RH).

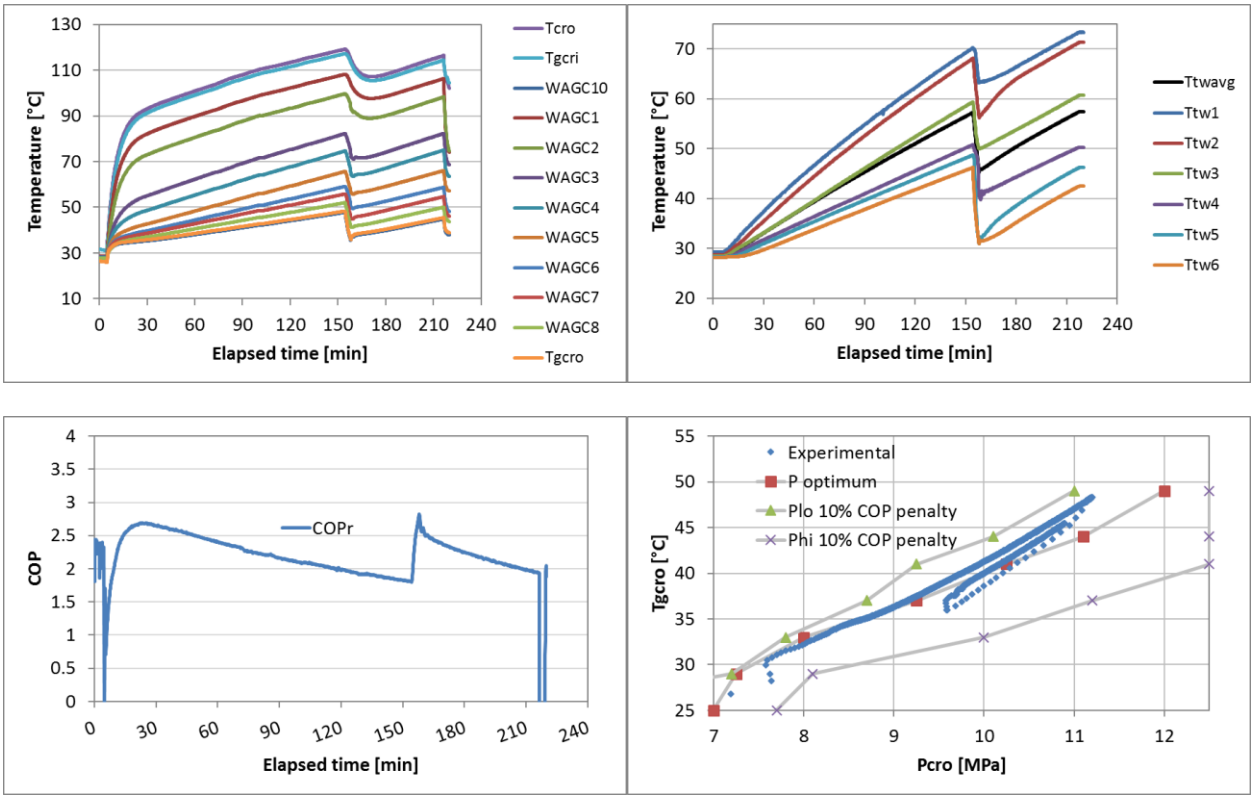

Figure 20. WAGC CO_2 temperatures, water tank temperatures, COP and compressor outlet pressure versus gas cooler outlet temperature for heat-up test (1,100 g charge) on 05/21/2014.

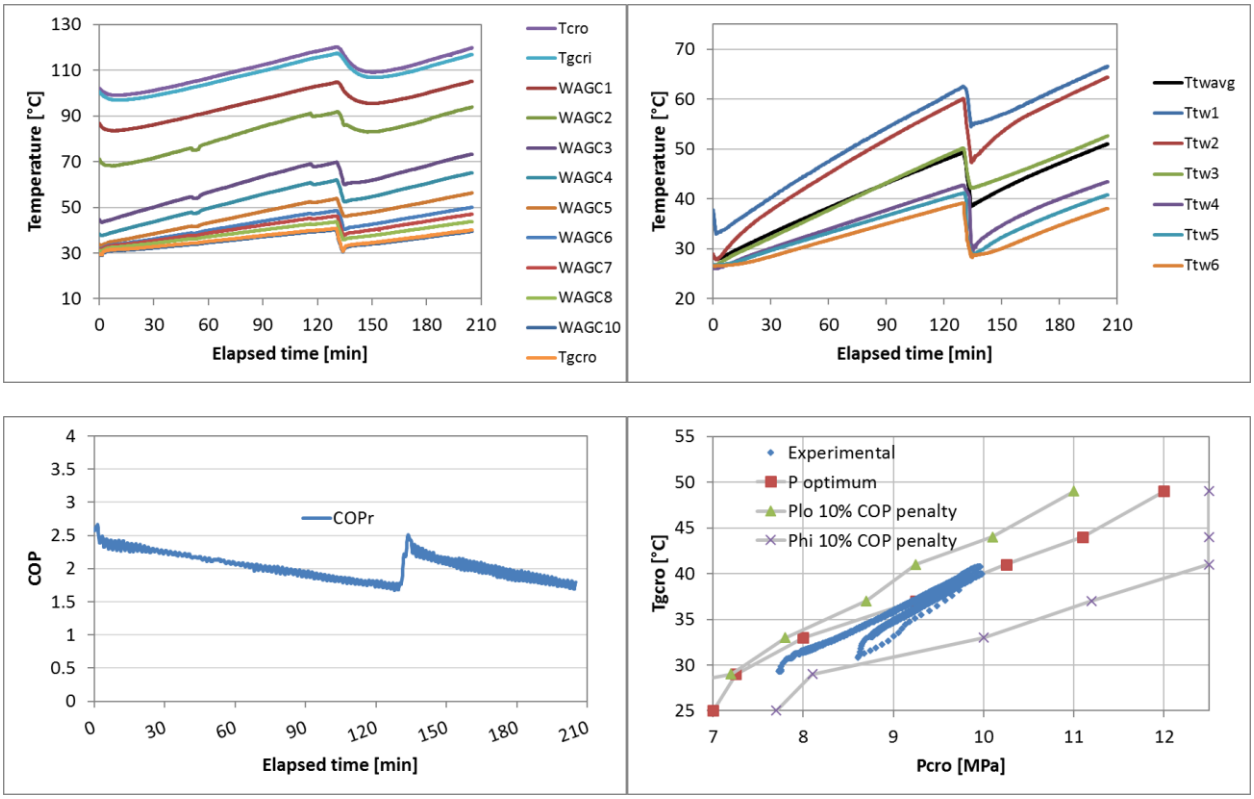

Figure 21. WAGC CO_2 temperatures, water tank temperatures, COP and compressor outlet pressure versus gas cooler outlet temperature for heat-up test (1,050 g charge) on 06/03/2014.

2.1.5.3 Generation 3b heat-up and EF tests

For the next generation CO_2 HPWH systems, the existing evaporator and IHX were removed and replaced with new units. The new evaporator was redesigned for higher superheat and fabricated by Super Radiator. It had the following specifications: 16 rows, 3 banks, 12.5 in. long tubes, 1 inlet and 1 outlet. The new IHX had the following specifications: annular diameters 0.5 in. × 0.035 in., and inner diameter 0.25 in., and 1.25 ft long. A new evaporator fan was installed (Sofasco model D28080V24HBM-P, 11 in. diameter, nominal 580 actual cubic feet per meter) and a new auxiliary heater was installed at the top of the water tank (3.6 kW, Backer model SG1353-430326). A mixing valve was added at the tank outlet (Watts model LF1170-UT-M2 3/4 in.) and the tank was further insulated (0.5 in. added, Armacell Flex Microban, 1.5 in. total). The results of a heat-up test conducted on 12/17/2014 and subsequent EF test on 12/18/2014 are shown below (Figures 22–24).

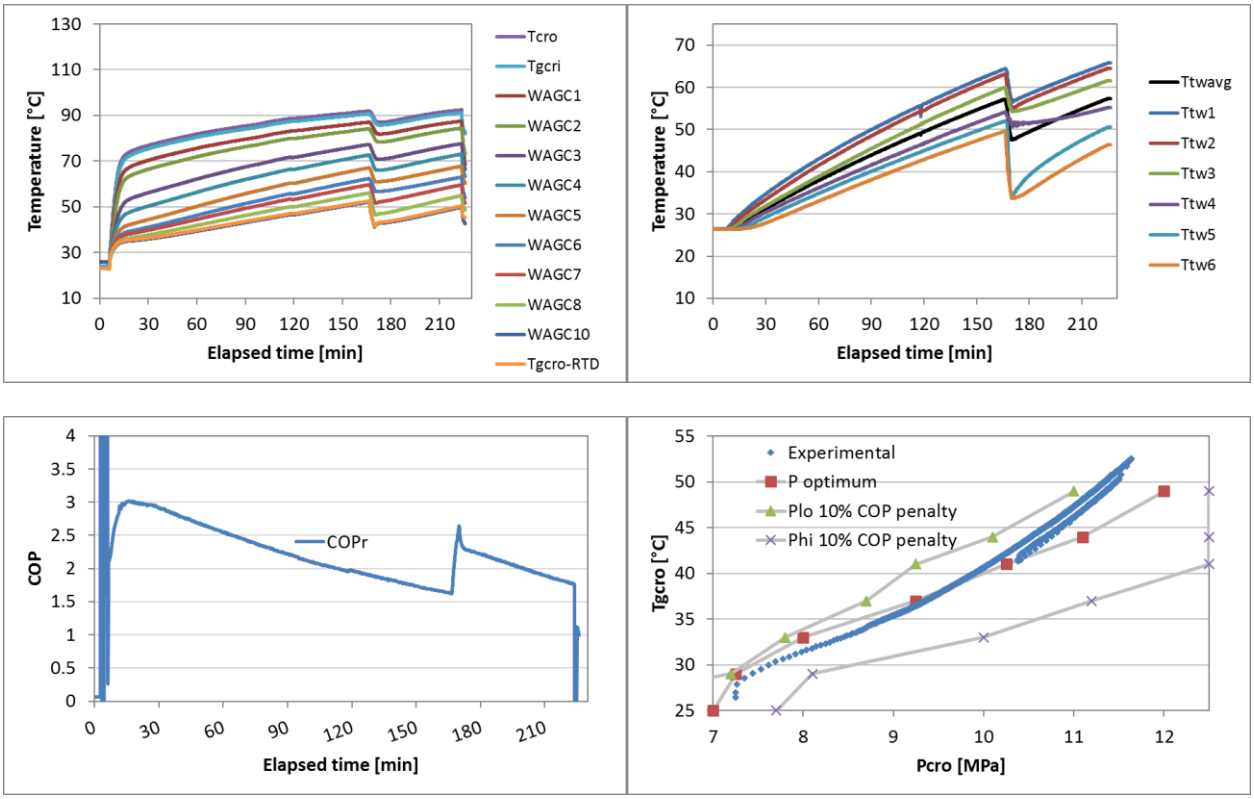

Figure 22. WAGC CO_2 temperatures, water tank temperatures, COP and compressor outlet pressure versus gas cooler outlet temperature for heat-up test (1,205 g charge) on 12/17/2014.

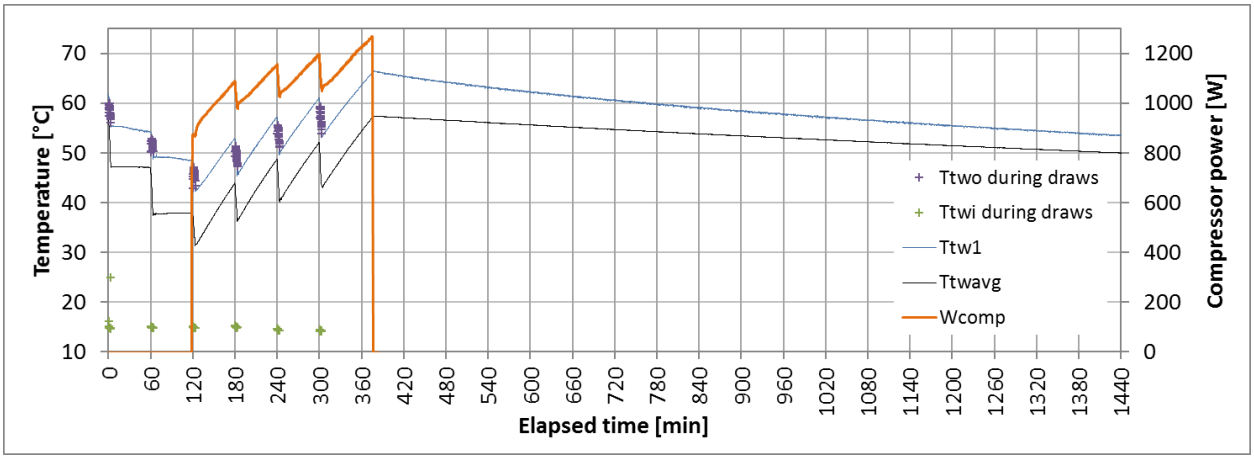

Figure 23. Water temperatures and compressor power for EF test on 12/18/2014 (EF = 1.986).

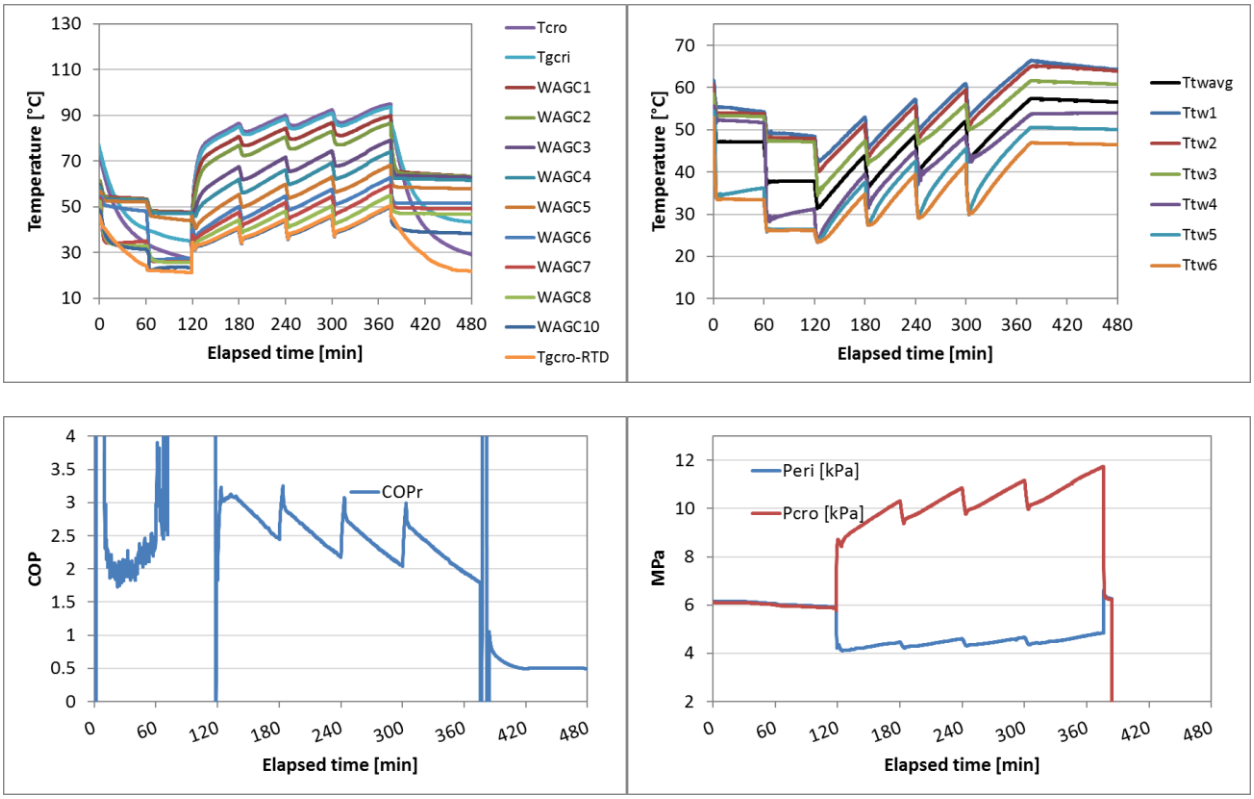

Figure 24. WAGC CO_2 temperatures, water tank temperatures, COP and compressor outlet/evaporator inlet pressures for EF test on 12/18/2014 (EF = 1.986).

2.1.5.4 Generation 3b FHR and UEF tests

In anticipation of the new uniform energy factor (UEF) test procedures (10 CFR 43), first hour rating (FHR) tests were conducted yielding an FHR of 73.5 gal. Temperatures (water and CO_2) and compressor power for the test on 02/13/2015 are shown below (Figure 25 and Figure 26).

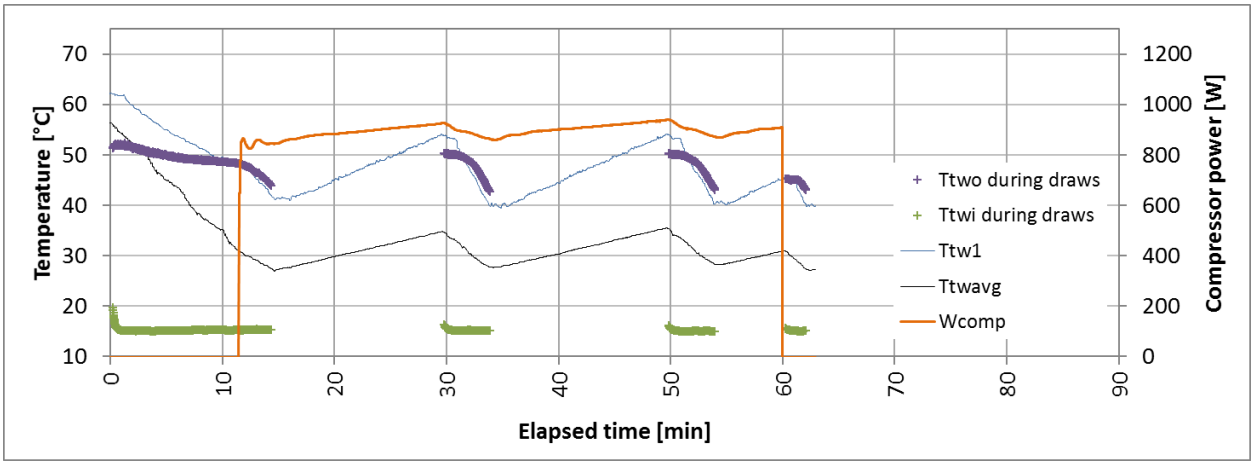

Figure 25. Water temperatures and compressor power for FHR test on 02/13/2015.

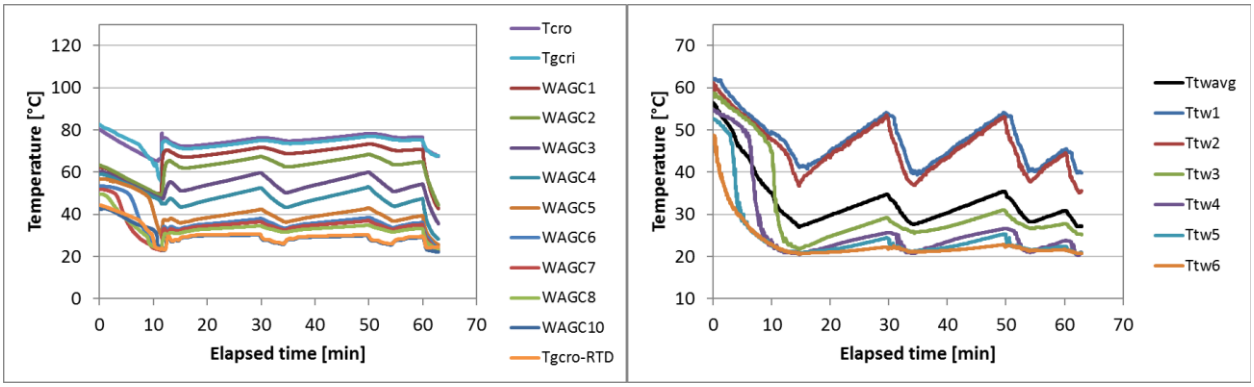

Figure 26. WAGC CO_2 temperatures and water tank temperatures for FHR test on 02/13/2015.

The FHR result indicated that a medium usage draw pattern was to be used for subsequent UEF testing on this unit. The first UEF test was conducted on 02/24/2015. Although some measured quantities were slightly out of range (total volume of water drawn, water draw flow rate) from those specified in the test procedure, the test was successful and yielded UEF = 2.11 (Figure 27 and Figure 28).

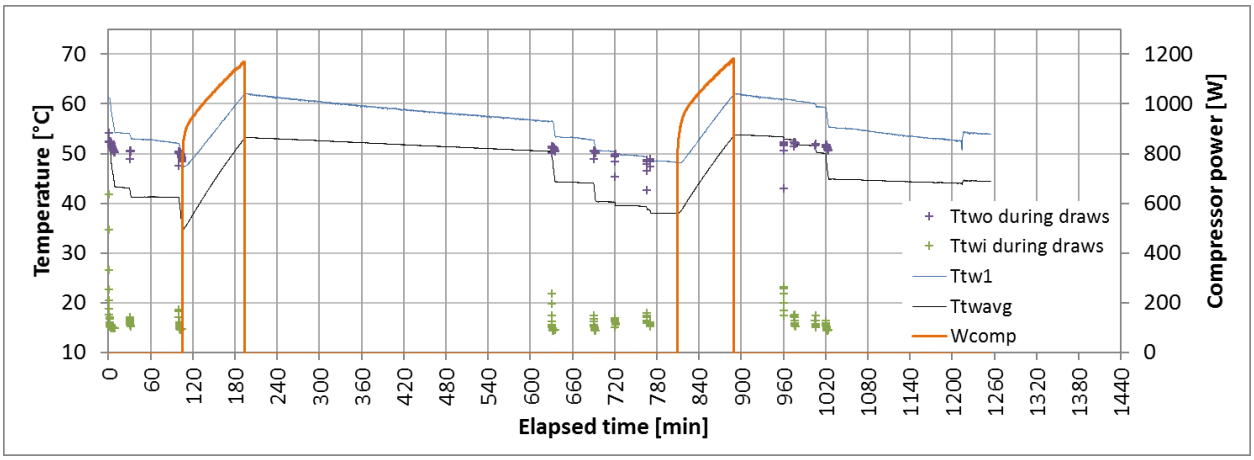

Figure 27.Water temperatures and compressor power for UEF test on 02/24/2015 (UEF = 2.11).

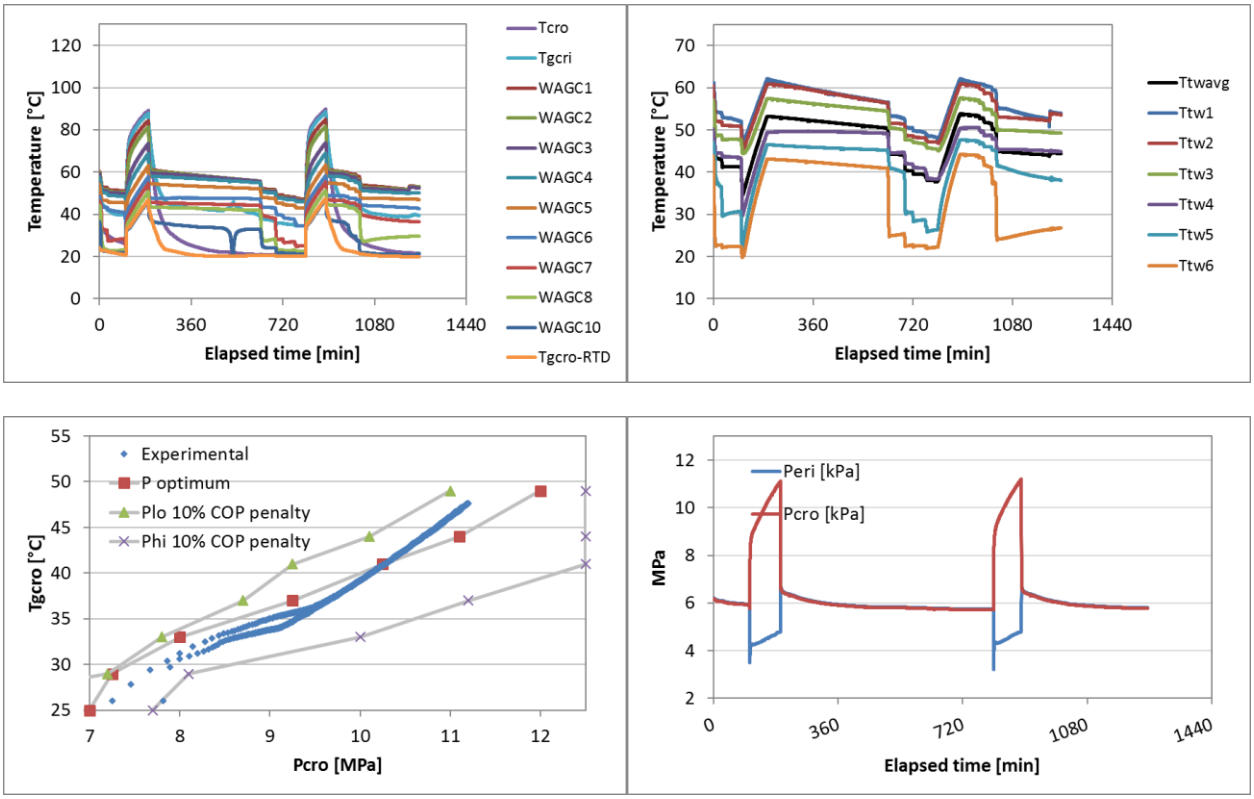

Figure 28. WAGC CO_2 temperatures, water tank temperatures, compressor outlet pressure versus gas cooler outlet temperature and compressor outlet/evaporator inlet pressures for UEF test on 02/24/2015 (UEF = 2.11).

2.2 ABSORPTION HPWH

The basis of energy savings for gas HPWHs is illustrated in Figure 29 and Figure 30. By combusting fuel on site to drive a thermally-activated heat pump, the device can use ambient heat and deliver a primary energy ratio that is even higher than electric heat pump water heaters.

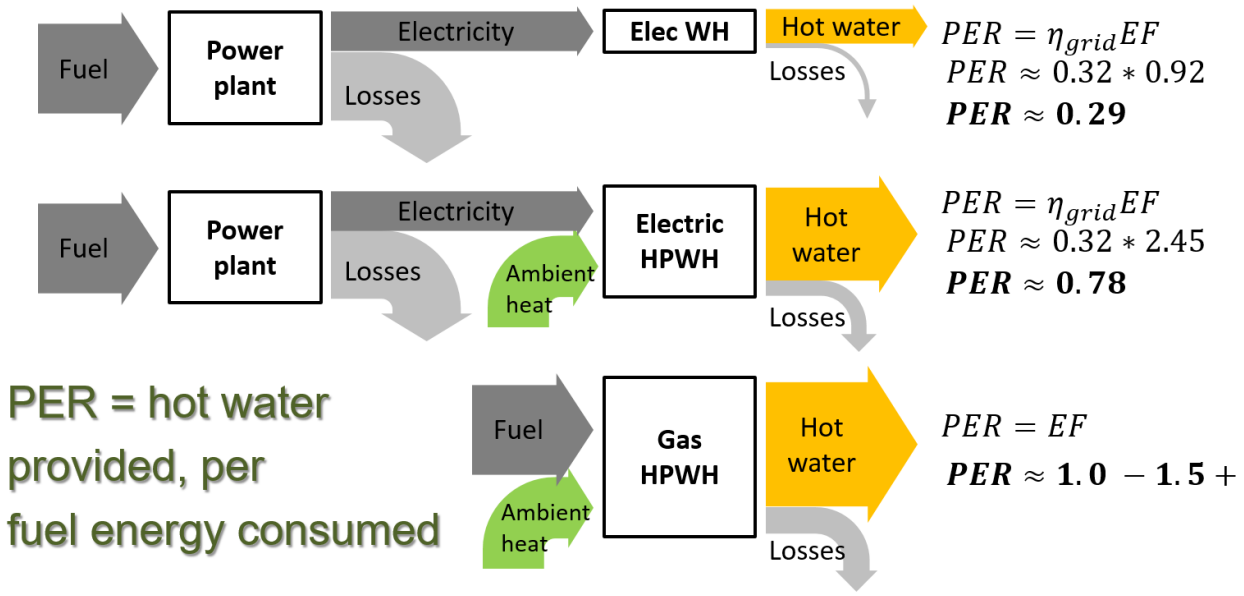

Figure 29. Energy savings for gas heat pump water heaters.

The primary energy saving potential of gas HPWHs is the highest of any water heating technology, but research and development is required to resolve cost and novelty barriers.

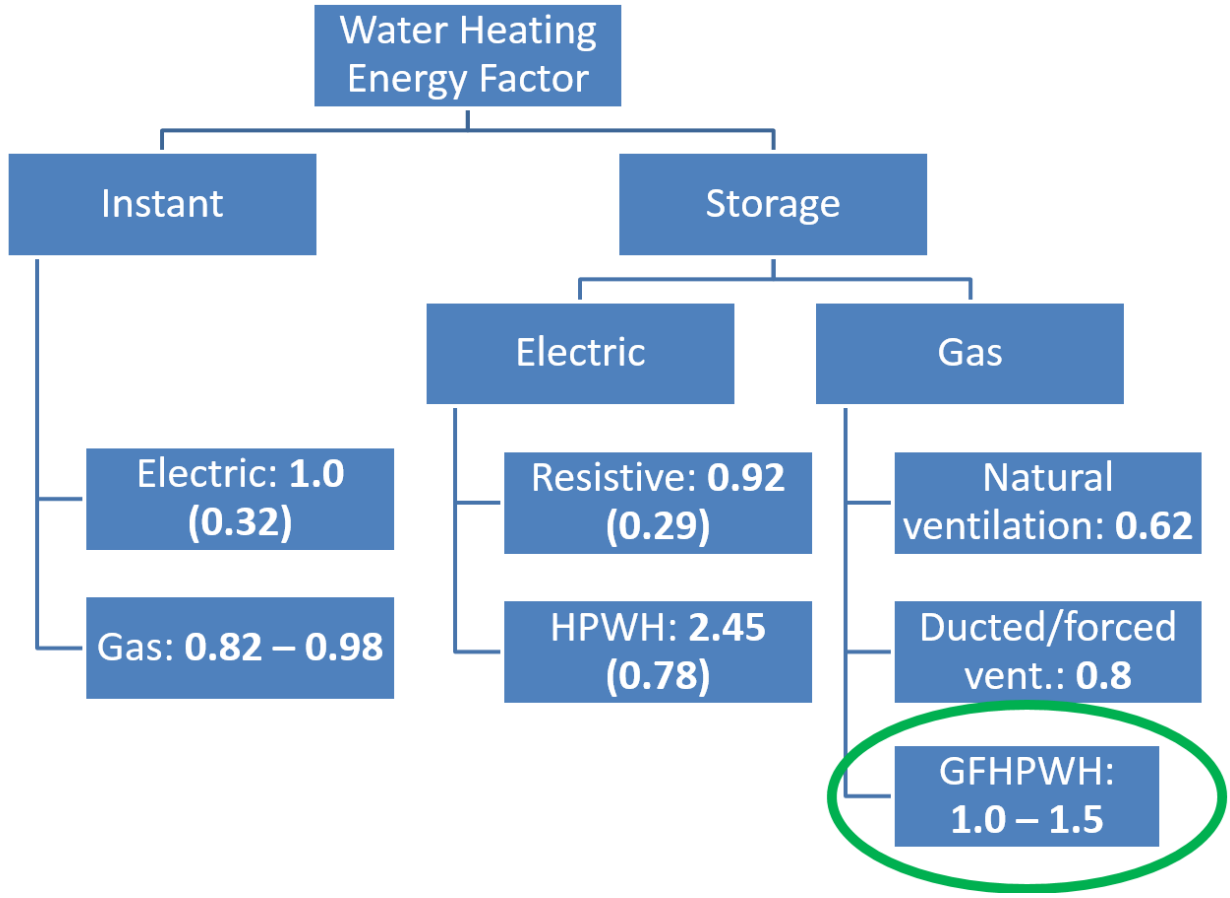

Figure 30. Site and source EF for various water heating technologies.

The cost challenge is portrayed in Figure 31. Given the dramatically low cost requirements for favorable payback (cost premium of ≤$300 for ≤5 y payback, per Figure 32) the team decided that the conventional falling film absorber configuration was not feasible from a cost perspective. This project did not investigate ammonia/water-based absorption for residential water heating because that technology was supported by DOE in a separate project.

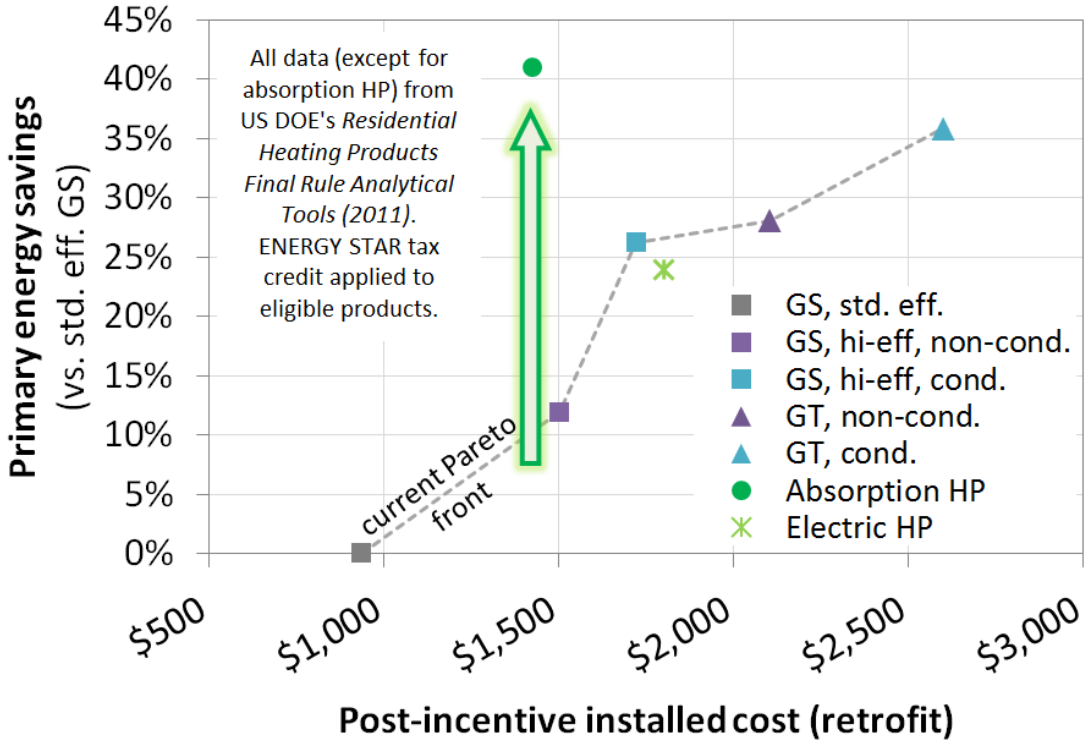

Figure 31. Absorption HPWH technology has the potential to leapfrog the existing Pareto set of technologies by maximizing savings and minimizing installed retrofit cost.

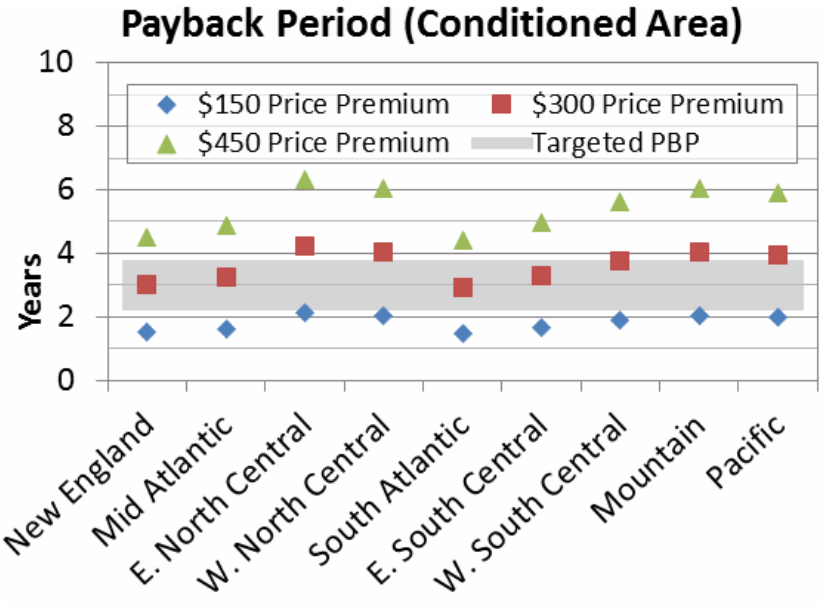

Figure 32. The payback period for a $300 postincentive installed cost premium is favorable in many regions of the United States.

A novel flow configuration for an absorption HPWH cycle with solution HX was investigated. Figure 33 to Figure 35 illustrate the progression from a conventional absorption heat pump cycle to the novel approach. Figure 36 illustrates a further innovation based on a semi-open flow circuit that eliminates the evaporator component developed under this project. Figure 37 illustrates some of the key advantages for the semi-open flow circuit employing an ionic fluid. The ionic fluid development is discussed in the following section. More details on the semi-open flow circuit development are given in section 2.2.4.

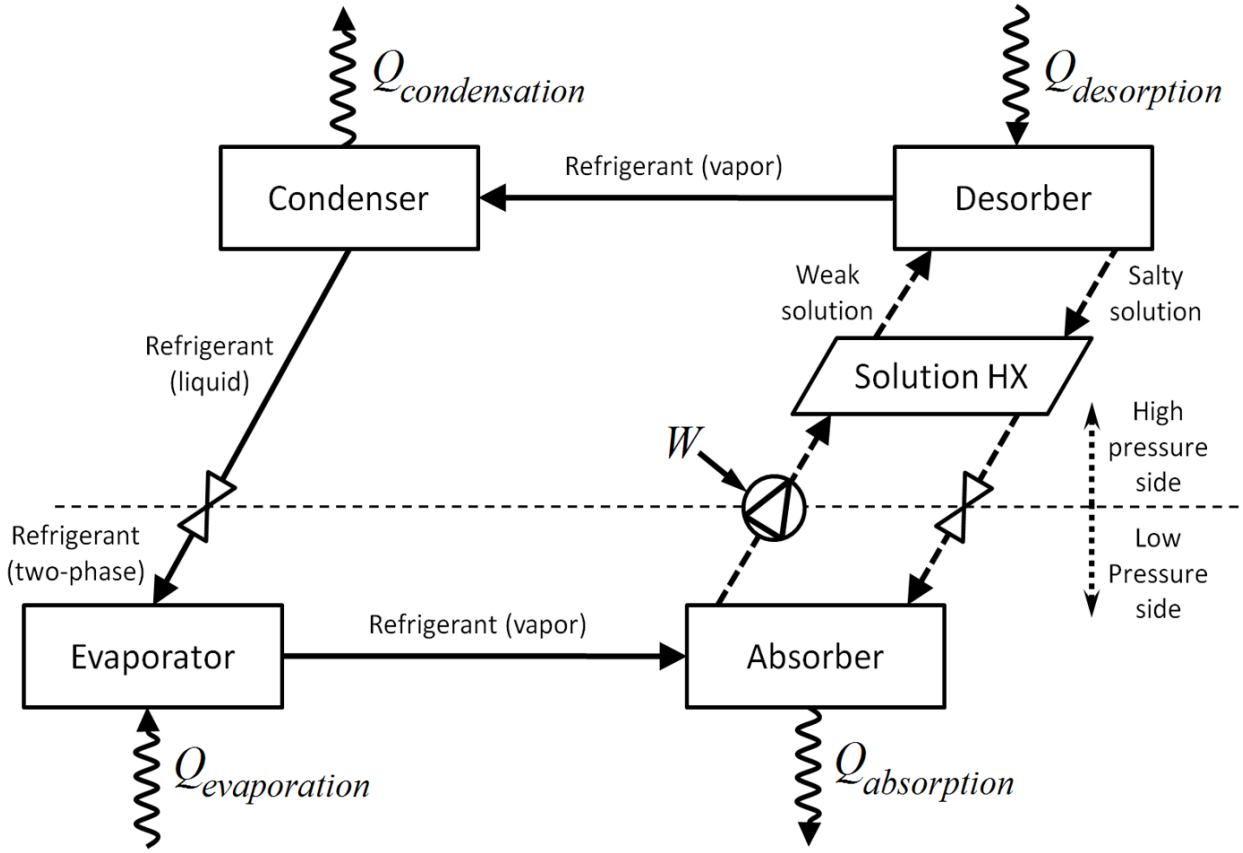

Figure 33. The conventional absorption process flow involves a solution HX transferring heat from the salty solution to the dilute, weak solution.

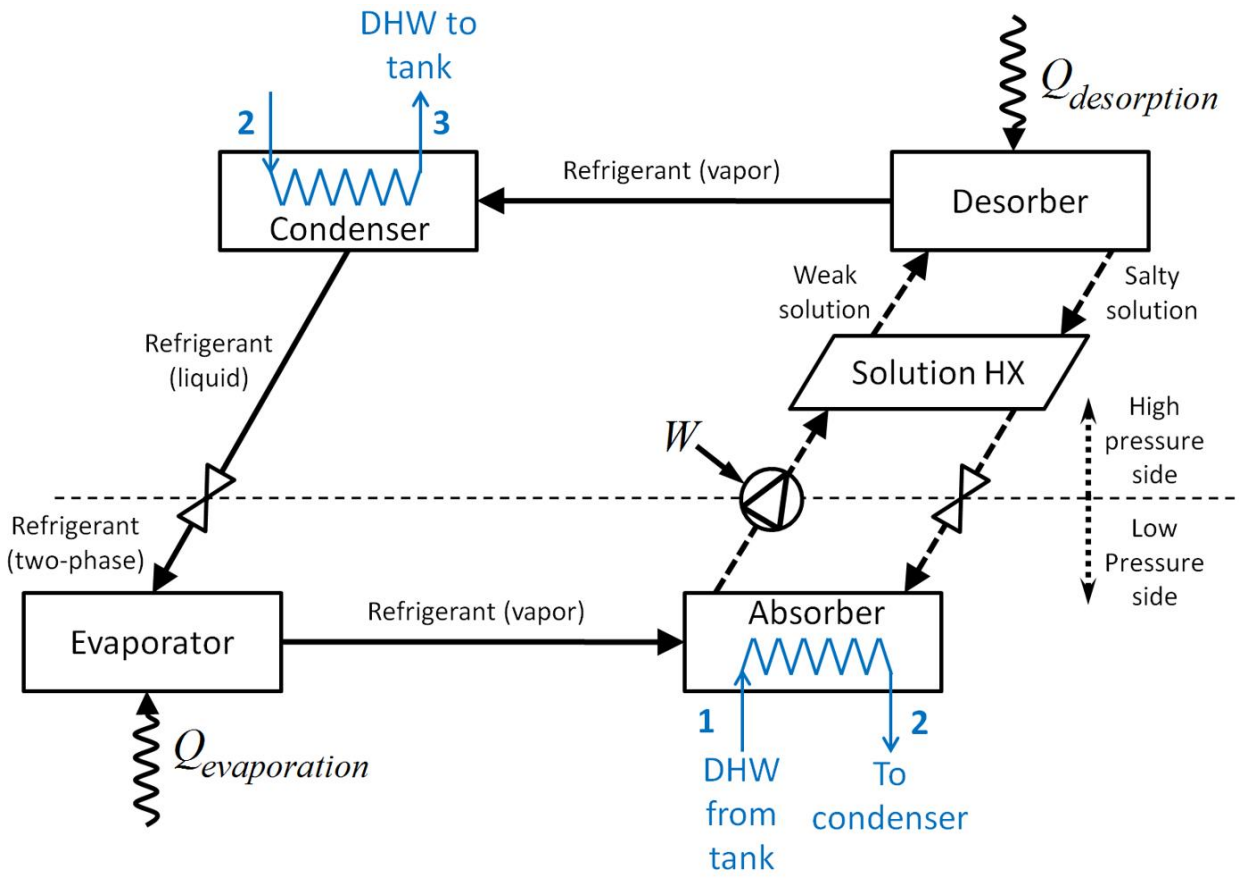

Figure 34. The ideal process flow for an absorption water heater typically involves cooling the absorber and condenser in series, with the condenser operating at the higher temperature.

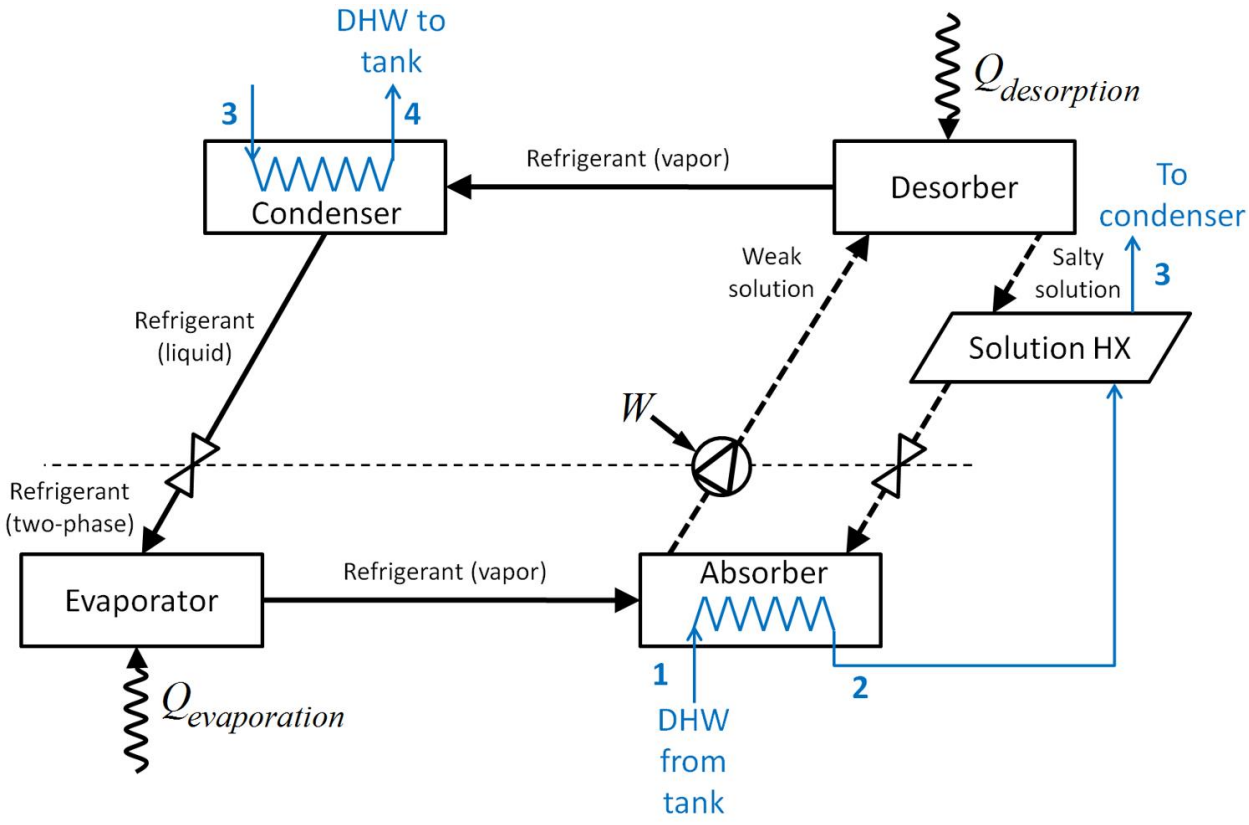

Figure 35. In a novel configuration, the process flow was modified so the hot solution heats the process water directly, which serves to lower the absorber temperature as much as possible. The weak solution is not preheated before entering the desorber, which also improves the usable glide in the desorber, potentially improving combustion efficiency.

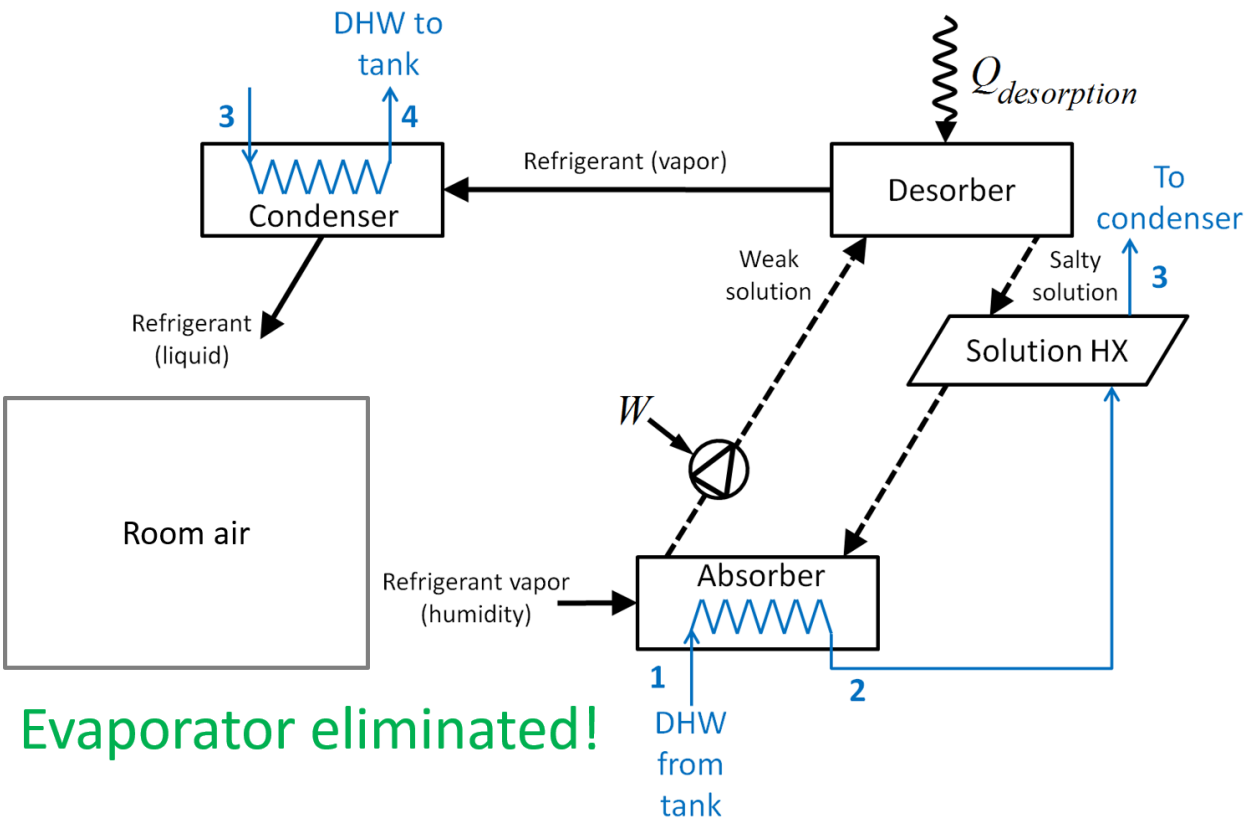

Figure 36. In the novel semi-open architecture, the evaporator component is eliminated. Instead the absorber sources water vapor from humidity in the surrounding air, and the condenser discharges liquid water to a drain or an evaporative cooler.

Challenge	Open membrane-based system
Sensitivity to vacuum leaks	✓ Operate at atmospheric pressure
Crystallization	✓ Ionic liquid
Corrosion (generation of non-condensables)	✓ Ionic liquid
High viscosity of ionic liquids	✓ Microstructure-enhanced mass transfer

Figure 37. The semi-open membrane-based ionic liquid absorption system addresses key challenges faced by absorption heat pump water heating technology.

2.2.1 Glycol-Based Anticrystallization Additive

The empirical equation of state provided in *ASHRAE Fundamentals* for water/LiBr mixtures was used as a functional form for an equation of state of water/LiBr/1,2-propanediol mixtures. An optimization was carried out with the eight parameter values as design variables. To ensure a thermodynamically consistent result, the objective function was a weighted composite of two elements. The first was the simple sum of squared errors in predicted refrigerant saturation temperature corresponding to the predicted vapor pressure for a given X and Tsoln. The second was an index of the nonlinearity in isostere slopes in a Clapeyron diagram. The index included nonlinearity as X changes (constant T) and nonlinearity as T changes (constant X).

Equipped with an EOS for each novel mixture, it becomes possible to plot the solubility on a Dühring diagram. For a novel mixture to have a chance at beating plain LiBr, its solubility line must lie below the LiBr solubility line on the Dühring diagram (Figure 38).

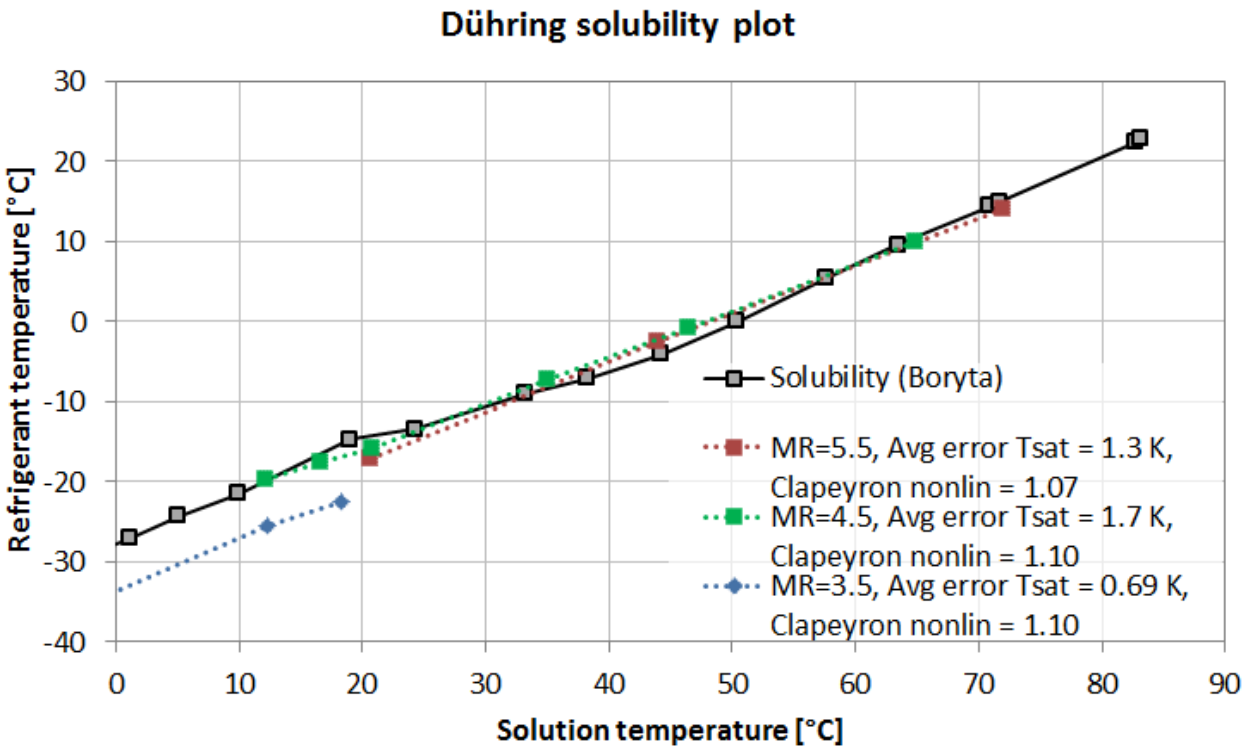

Figure 38. Dühring solubility figure for the three mass ratios of 1,2-propanediol investigated.

2.2.2 Operational Strategies to Avoid Crystallization

There are a few important situations to avoid during startup and shutdown (

Table 4). These are crystallization after shutdown, crystallization at startup, mixing of the stratified tank at startup, and mixing of stratified tank during dilution cycle.

Table 4. Operational crystallization challenges

Potential problem	Resolution of problem
Crystallization after shutdown	Dilution cycle
Crystallization at startup	Dilution cycle at previous shutdown; sufficient solution flow rate; low initial DHW flow rate
Mixing of stratified tank at startup	Low or zero initial DHW flow rate until absorber and condenser are hot
Mixing of stratified tank during dilution cycle	Carefully timed DHW flow shut off

Note: DHW = domestic hot water

Crystallization can occur on shutdown if highly concentrated solution is allowed to cool toward ambient temperature. This can be avoided by a "dilution cycle." During the dilution cycle, the burner is shut off, but the solution pump continues operating. The domestic hot water (DHW) continues flowing to cool the absorber, but it must be turned off once the outlet temperature from the condenser threatens to overturn the stratified tank. The evaporator fan runs on high to evaporate as much refrigerant as possible and push it into solution. Once the DHW flow stops, the solution pump runs until the absorber solution outlet temperature is stable. At this point, no further dilution occurs.

For absorption heat pumps operating in heating mode, the dilution cycle has the benefit of priming the solution for more rapid startup. This is not true for absorption chillers, which have delayed evaporator startup performance as a result of the dilution cycle.

Crystallization can also occur during startup if too much desorption occurs in the desorber. This may be caused by a low condenser temperature, too high of an initial firing rate, or too low of an initial solution flow rate through the desorber. The highly concentrated solution formed in the desorber is then overly cooled by the very cool solution on the other side of the solution HX. So startup crystallization can be avoided by a combination of (1) proper dilution at the previous shutdown, (2) not overcooling the condenser at startup, (3) not overcooling the absorber at startup, and (4) ensuring sufficient solution flow through the desorber.

2.2.3 HVAC Burden

Heat pumps extract heat from their surroundings. When a heat pump is located indoors, it cools the air in the building, which can be a drawback during the heating season. This has been called the "HVAC burden" of HPWH operation. Field easurements have shown despite the HVAC burden of electric HPWHs, the overall effect on whole-building consumption is still net positive (Munk 2012). Gas-fired HPWHs have the advantage of a lower HVAC burden for a given heating load (Figure 39).

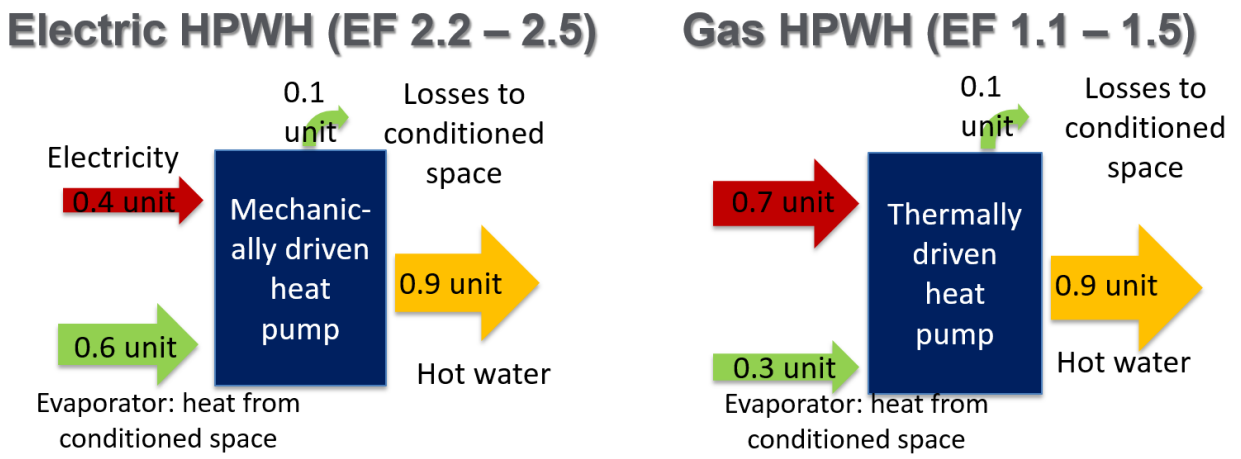

Figure 39. The amount of heat drawn from the conditioned space, or HVAC burden, of electric (*left*) HPWHs is much greater than for gas (*right*) units.

The normalized HVAC burden can be expressed analytically as

$$normalized\ HVAC\ burden = \frac{Q_{evap}}{Q_{HW}} = 1 - \frac{1}{EF},$$

where the EF is defined as hot water delivered per unit site energy consumed (consistent with the DOE definition for both gas and electric HPWHs). This is also shown in Figure 40. The space cooling burden of the gas HPWH is 2–4 times lower than for the electric HPWH. In addition, less volumetric air flow is required by the gas HPWH evaporator compared with the electric HPWH evaporator, leading to the potential for less noise, less "cold blow" effect, and the ability to be installed in smaller rooms. Consequently, the gas system is more suitable for semiconditioned spaces in cold climates.

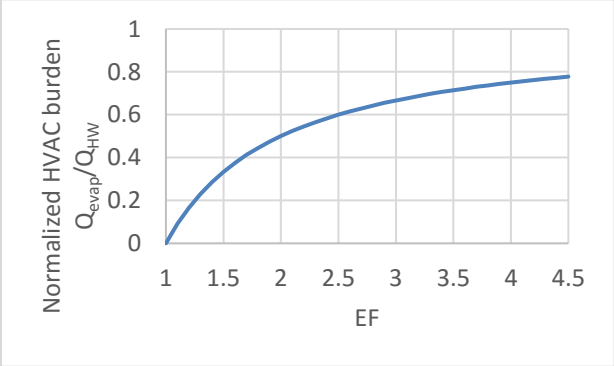

Figure 40. HVAC burden of HPWHs as a function of EF.

2.2.4 Prototype Development

A series of successive prototypes were developed. The first prototype was based on water/LiBr technology and sought to resolve the crystallization problems common to these systems by identification and characterization of a newly promising additive, 1,2 propanediol (Figure 41). This prototype suffered from insufficient absorber capacity, difficulty in priming the solution lines, and controlling the solution flow rates. After multiple generations of absorbers and plumbing configurations, the ORNL team resolved

the priming and control issues. However, the poor absorber performance remained a barrier to achieving an acceptable cycle COP, even for the third generation absorber.

Figure 41. Prototype based on water/LiBr in an ORNL lab.

The second generation absorber was designed as shown in Figure 42. The tubes used were treated with a sandblasted water jet medium to enhance wettability. This choice was made based on a sample of surface treatments (Figure 43).

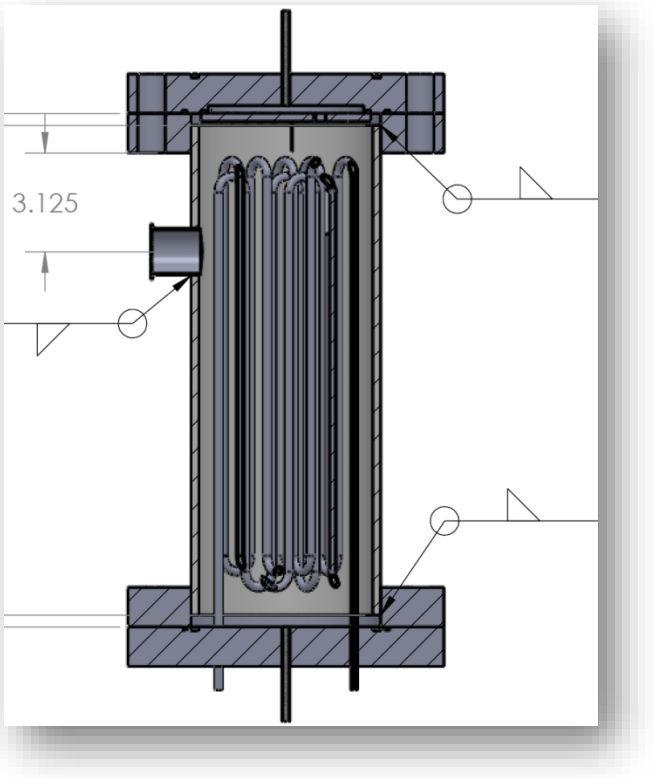

Figure 42. Drawing of revised absorber used in 2nd generation water/LiBr prototype.

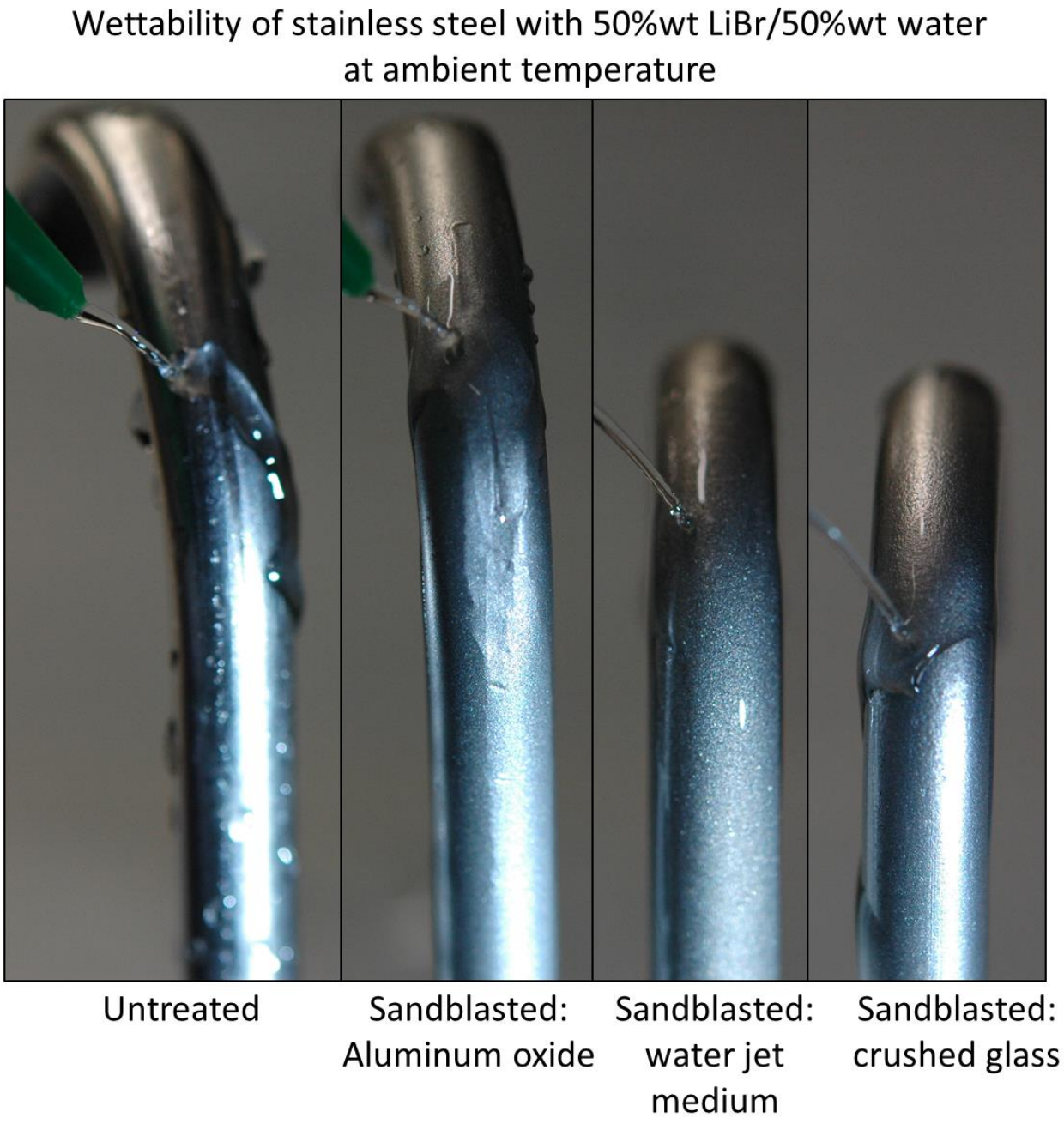

Figure 43. Investigation of stainless steel surface treatments to maximize wettability with salt solution. The sandblasting with water jet medium produced the highest wettability.

Figure 44. Last generation water/LiBr prototype. The shared condenser/desorber vessel was split. The condenser is on top and connected to the desorber by a hose.

In the final prototype generation, the condenser was moved out of the desorber vessel to prevent solution contaminating the condenser, the solution HX was eliminated to improve solution flow, and component thermal masses were reduced (Figure 44).

The last configuration of the prototype was able to heat a tank of water but only at an unacceptably poor COP of around 1 because of the very low absorber capacity (Figure 45).

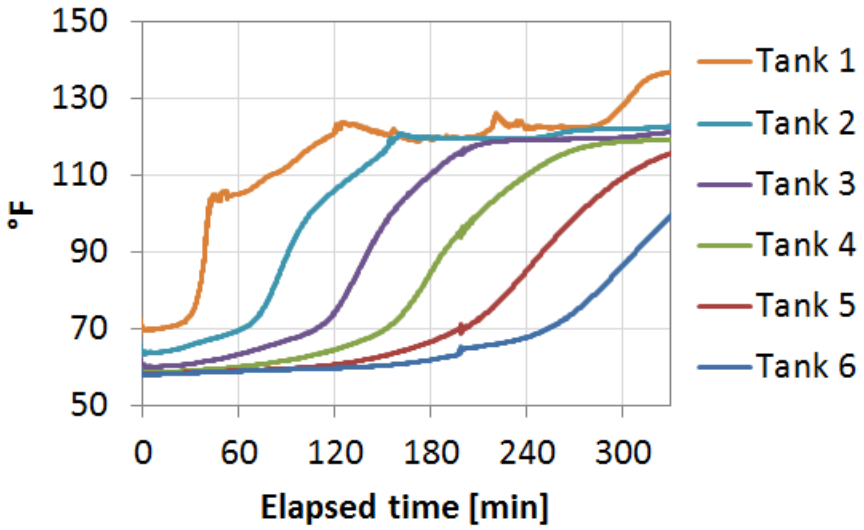

Figure 45. Tank temperatures during experimental heat up test with water/LiBr absorption prototype.

The new 1,2-propanediol additive was shown to have merit, but it did not fully resolve the crystallization challenges. Next the team pursued ionic liquids as an alternative to LiBr working fluids. Subcontracts were established with Ionic Research Technologies to identify promising ionic liquids through molecular dynamics simulations and with University of Florida to explore membrane-based cycle configurations that could help deal with the inherent problems associated with ionic liquids, such as their high viscosity. In the course of exploring these membrane-based cycles, the team discovered a semi-open configuration with the potential for dramatically lower cost.

Because of difficulties in achieving sufficient absorber capacity and the anticipated difficulties of maintaining vacuum over the service life of the appliance, a new approach was taken in the last year of the project. The focus shifted to the "semi-open" absorption cycle that does not require subatmospheric pressures. In this configuration, a membrane separates the solution from air, and the absorber removes humidity from the surrounding air. An early partial-scale prototype of this system is shown in Figure 46.

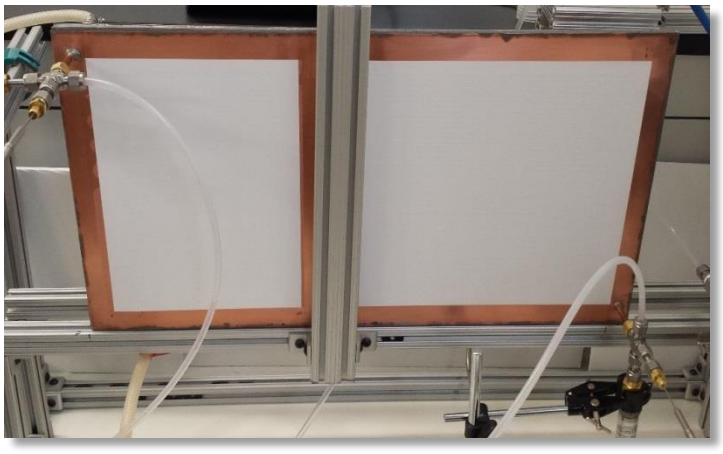

Figure 46. Membrane surface of condenser (*left*) and absorber (*right*).

Another benefit of the membrane-constrained architecture is the ability to use surface enhancements to improve the mass transfer through the solution (Figure 47).

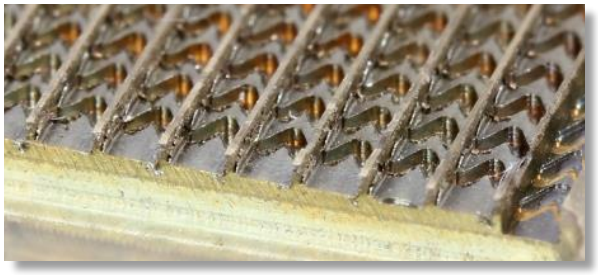

Figure 47. Example pattern used to promote laminar mixing of the solution to enhance mass transfer.

Figure 48 depicts the working principle of the semi-open absorption cycle.

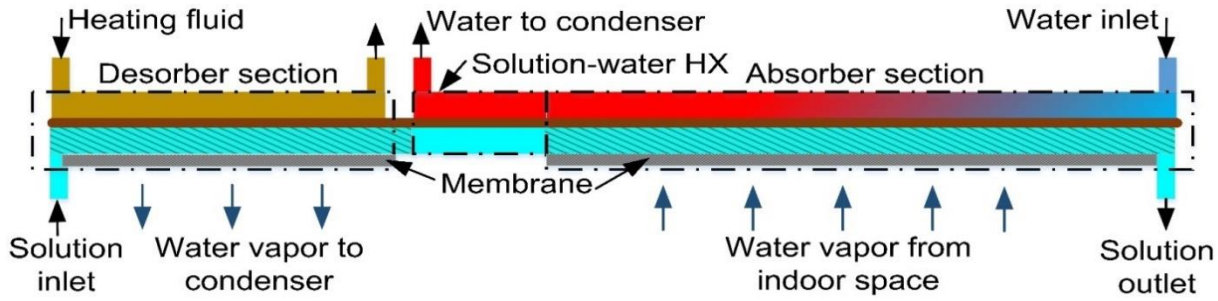

Figure 48. Cross section of semi-open absorption architecture.

The theory behind the newly termed "semi-open" natural gas-fired design reduces the cost and complexity of traditional closed gas-fired systems by streamlining the mechanical design, and eliminating the evaporator component. The physically simpler semi-open system operates at the surrounding atmospheric pressure, eliminating the need for a vacuum pump to purge gas build up, and allowing the use of an inexpensive, non-sealed solution pump. It also allows manufacturers to consider lower-cost, lightweight polymers instead of costly, bulkier metals to build equipment, resulting in less susceptibility to corrosion. These advantages are summarized in Table 5.

Table 5. Advantages of semi-open sorption systems

Component	**Traditional closed sorption**	**Semi-open sorption**
Vessel materials	Carbon steel	Polymer
Solution pump	Hermetic, with hydrostatic plus 1–15 kPa variable head	Nonhermetic with constant hydrostatic head
Vacuum requirements	Periodic vacuum pumping	None
Vessel pressure rating	Must withstand full vacuum (34 ft)	Only hydrostatic pressure differentials (~2 ft)
Evaporator	Required	Not required

As of the end of this project, the semi-open system appeared promising. Separate funding is in place to allow follow-on work to evaluate this technology more thoroughly.

3. INVENTIONS AND COMMUNICATIONS

Inventions

1. Moghaddam, S., Chugh, D., Nasr Isfahani, R., Bigham, S., Fazeli, A., Yu, D., Mortazavi, M., and Abdelaziz, O. (2013). Open Absorption Cycle for Combined Dehumidification, Water Heating, and Evaporating Cooling. US Patent application UF-14820.

2. Abdelaziz, O., Vineyard, E., and Zaltash, A. (2010). "Absorption Heat Pump System and Method of Using the Same." US Patent application 12/829,940, filed July 2, 2010. UT-Battelle ID 201002389.

Communications

Journal Publications

1. Gluesenkamp, K., Chugh, D., Abdelaziz, O., and Moghaddam, S. (in press). "Efficiency Analysis of Semi-Open Sorption Heat Pump Systems." *Renewable Energy*, Accepted.

2. Wang, K., Abdelaziz, O., Kisari, P., and Vineyard, E. (2011). "State-of-the-Art Review on Crystallization Control Technologies for Water/LiBr Absorption Heat Pumps." *International Journal of Refrigeration* 34: 1325–37.

3. Wang, K., Abdelaziz, O., and Vineyard, E. (2011). "The Impact of Water Flow Configuration on Crystallization in LiBr/H_2O Absorption Water Heater." *International Journal of Energy Technology and Policy* 7: 393–404.

Conference Papers

1. Gluesenkamp, K. (2016). "Energy Factor Analysis for Gas Heat Pump Water Heaters." *ASHRAE Annual Meeting 2016*, June 29, St. Louis, MO.

2. Gluesenkamp, K., and Bush, J. (2016). "Impact on Water Heater Performance of Heating Methods that Promote Tank Temperature Stratification." *ASHRAE Annual Meeting 2016*, June 29, St. Louis, MO.

3. Chugh, D., Isfahani, R. N., Gluesenkamp, K., Abdelaziz, O., and Moghaddam, S. (2015). "A Hybrid Absorption Cycle for Water Heating, Dehumidification, and Evaporative Cooling." Proceedings of the ASME InterPACKICNMM2015, July 6–9, San Francisco, CA.

4. Chugh, D., Nasr Isfahani, R., Gluesenkamp, K., Abdelaziz, O., and Moghaddam, S. (2014). "A Novel Absorption Cycle for Combined Water Heating, Dehumidification and Evaporative Cooling." *International Sorption Heat Pump Conference*, March 31–April 3, College Park, MD.

5. Maerzke, K., Mozurkewich, G., Abdelaziz, O., Gluesenkamp, K., Schneider, W., Morrison, D., and Maginn, E. (2014). "Ionic Liquid Development for Absorption Heat Pump Applications." *International Sorption Heat Pump Conference*, March 31–April 3, 2014, College Park, MD.

6. Kisari, P., Wang, K., Abdelaziz, O., and Vineyard, E. (2010). "Crystallization Temperature of Aqueous LiBr Solutions at Low Evaporation Temperature." *Road to Climate Friendly Chillers*, Cairo, Egypt.

7. Wang, K., Kisari, P., Abdelaziz, O., and Vineyard, E. (2010). "Testing of Crystallization Temperature of a New Working Fluid for Absorption Heat Pump Systems." *Road to Climate Friendly Chillers*, Cairo, Egypt.

Presentations and Other Communications

1. Gluesenkamp, K., de Almeida, V., and Abdelaziz, O. (2016). "Affordable ENERGY STAR® Residential CO_2 HPWH for the US Market." Presented to 2013 ACEEE Hot Water Forum, February 22, Portland, OR.

2. Gluesenkamp, K., and Vineyard, E. A. (2015). "Semi-Open Sorption Systems as Heat Pumps and Coolers." Presented to Sorption Friends, September 22, Milazzo, Italy.

3. Gluesenkamp, K. (2015). "Fuel-Fired Heat Pump Water Heaters: A Generalized Design Study." Presented to Sorption Friends, September 22, Milazzo, Italy.

4. Gluesenkamp, K. (2015). "US Activities, Test Standards and Field Tests in Gas-Fired Heat Pump Water Heaters." Presented to 4th Expert Meeting of the IEA HPP Annex 43, June 9, Vienna, Austria.

5. Gluesenkamp, K. (2015). "Development of Low-Cost ENERGY STAR®-Qualified Residential CO_2 HPWH Prototype." Presented to ACEEE Hot Water Forum, February 23, Nashville, TN.

6. Gluesenkamp, K. (2014). "US Activities in Gas-Fired Heat Pump Water Heaters." Presented to 3rd Expert Meeting of the IEA HPP Annex 43, November 6, Freiburg, Germany.

7. Gluesenkamp, K. (2014). "Gas-Fired Heat Pump Water Heaters." Presented to ASHRAE Annual Meeting 2014, July 2, Seattle, WA.

8. Gluesenkamp, K., Garrabrant, and M., Chapman, G. (2014). "Gas Heat Pumps: An Update" Webinar presented to Gas Committee of the Consortium for Energy Efficiency, March 20, 2014.

9. Gluesenkamp, K., Abdelaziz, O., and Vineyard, E. (2013). "Gas-Fired Absorption Heat Pump Water Heater Development at Oak Ridge National Laboratory." Presented to 2013 ACEEE Hot Water Forum, November 4, Atlanta, GA.

10. Gluesenkamp, K., Abdelaziz, O., and Vineyard, E. (2013). "Gas-Fired Absorption Heat Pump Water Heater Development at Oak Ridge National Laboratory." Presented to 2013 ACEEE Hot Water Forum, November 4, Atlanta, GA.

11. Abdelaziz, O., Maginn, E., and Morrison, D. (2013). "Ionic Fluid Design for Absorption Heat Pump Applications." Presented to Winter ASHRAE Conference, Seminar 58, Dallas, TX, USA.

12. Abdelaziz, O., Wang, K., Vineyard, E. A., and Roetker, J. "Development of Environmentally Benign Heat Pump Water Heaters for the US Market," 2012 ACEEE Summer Study on Energy Efficiency in Buildings, August 12–17, Pacific Grove, CA.

13. Sikes, K., Blackburn, J., and Abdelaziz, O. (2012). "Market Assessment for High-Performance Gas Absorption Water Heaters." November.

14. Brownell, D., Stevenson, A., and Guyer, E. (2011). "Absorption Heat Pump Water Heater Prototype, Design Report B." Submitted by Yankee Scientific Inc. to ORNL under subcontract number 4000101964, May 24.

15. Gluesenkamp, K., Vineyard, E.A. (2015). Participation in IEA Annex 43, "Fuel-Driven Sorption Heat Pumps for Heating Applications."

4. COMMERCIALIZATION POSSIBILITIES

As a result of the research conducted under this Cooperative Research and Development Agreement (CRADA), a path has been identified for a CO_2-based HPWH with the lowest possible price point meeting all ENERGY STAR criteria (for efficiency and first hour rating). Also, a viable path for a gas-fired HPWH at unprecedentedly low cost has been identified. Development work on this concept is continuing under a separately funded project.

5. REFERENCES

Department of Energy (2012). *2011 Buildings Energy Data Book.* March 2012. Available: http://buildingsdatabook.eren.doe.gov.

Munk, J. D., Baxter, V. D., and Gehl, A. C. (2012). "Measured Impact on Space Conditioning Energy Use in a Residence Due to Operating a Heat Pump Water Heater inside the Conditioned Space." *ASHRAE Transactions* 108 (2): 27–33.

US Code of Federal Regulations. (2015). Title 10: "Energy;" Part 430, "Energy Conservation Program for Consumer Products;" Subpart B, "Test Procedures;" Appendix E, "Uniform Test Method for Measuring the Energy Consumption of Water Heaters." 10 CFR 430.

U.S. Department of Energy. (2010). *Residential Heating Products Final Rule Technical Support Document.* Retrieved August 2011, from Appliances and Commercial Equipment Standards: http://www1.eere.energy.gov/buildings/appliance_standards/residential/heating_products_fr_tsd.html

U.S. Department of Energy. (2011, March). *Residential Heating Products Final Rule Analytical Tools.* Retrieved August 2011, from Final Rule Analytical Spreadsheets: http://www1.eere.energy.gov/buildings/appliance_standards/residential/heating_products_fr_spreadsheets.html